HHS Public Access

Author manuscript

Nat Immunol. Author manuscript; available in PMC 2016 March 01.

Published in final edited form as:

Nat Immunol. 2015 September ; 16(9): 980–990. doi:10.1038/ni.3226.

LEF-1 and TCF-1 orchestrate T follicular helper cell differentiation by regulating differentiation circuits upstream of Bcl6

Youn Soo Choi[1,^], **Jodi A. Gullicksrud**[2,3,^], **Shaojun Xing**[2], **Zhouhao Zeng**[4], **Qiang Shan**[2], **Fengyin Li**[2], **Paul E. Love**[5], **Weiqun Peng**[4], **Hai-Hui Xue**[2,3,*], and **Shane Crotty**[1,*]

[1]Division of Vaccine Discovery, La Jolla Institute for Allergy and Immunology, La Jolla, CA 92037

[2]Department of Microbiology, Carver College of Medicine, University of Iowa, Iowa City, IA 52242

[3]Interdiscipilinary Immunology Graduate Program, Carver College of Medicine, University of Iowa, Iowa City, IA 52242

[4]Department of Physics, The George Washington University, Washington DC, 20052

[5]Section on Cellular and Developmental Biology, NICHD, NIH, Bethesda, MD 20892

Abstract

T follicular helper (T_{FH}) cells are specialized effector $CD4^+$ T cells that help B cells develop germinal centers and memory. However, the transcription factors that regulate T_{FH} differentiation remain incompletely understood. Here we report that selective loss of either *Lef1* (LEF-1) or *Tcf7* (TCF-1) resulted in T_{FH} defects, while deletion of *Lef1* and *Tcf7* severely impaired T_{FH} differentiation and germinal centers. Forced expression of LEF-1 enhanced T_{FH} differentiation. LEF-1 and TCF-1 coordinated T_{FH} differentiation by two general mechanisms. First, they established the responsiveness of naïve $CD4^+$ T cells to T_{FH} signals. Second, they promoted early T_{FH} differentiation via the multipronged approach of sustaining expression of IL-6Rα and gp130, enhancing ICOS expression, and promoting expression of Bcl6.

Keywords

Lymphoid enhancer factor (LEF)-1; T cell factor (TCF)-1; IL-6 receptor alpha (IL-6Rα); IL-6 signal transducer (gp130); inducible costimulator (ICOS); B cell lymphoma 6 (Bcl6); Prdm1; Blimp1

*Corresponding authors: Shane Crotty. shane@lji.org And Hai-Hui Xue. hai-hui-xue@uiowa.edu.
^These authors contributed equally

ACCESSION NUMBERS

Gene Expression Omnibus under accession numbers GSE66781 and GSE67336.

AUTHOR CONTRIBUTIONS

Y.S.C., J.A.G., S.X., F.L. and Q.S. performed the experiments and analyzed the data. Z.H. analyzed the RNA-seq data under supervision of W.P. P.E.L provided critical reagents. Y.S.C., S.C., and H.H.X. conceived the project and wrote the paper. S.C. and H.H.X. supervised the overall study.

The authors declare no conflicts of interest.

T cell help to B cells is a critical component of adaptive humoral immunity[1, 2]. During viral infections, the formation of germinal centers (GCs) by antigen (Ag)-specific B cells requires key signals provided by T follicular helper (T_{FH}) cells[3], resulting in the development of high-affinity long-lived plasma cells and memory B cells[4, 5]. T_{FH} differentiation begins outside of B cell follicles in a stepwise fashion. Early induction of key molecules of T_{FH} differentiation, such as Bcl6, CXCR5, ICOS, and PD-1, occurs in the T cell zone when $CD4^+$ T cells interact with Ag-presenting dendritic cells (DCs) or other antigen presenting cells (APCs), which then enable the migration of the activated $CD4^+$ T cells towards the border of B cell follicles. Upon recognition of cognate Ag-presenting B cells, the differentiating T_{FH} cells migrate deep inside B cell follicles and further differentiate into GC T_{FH} cells as they direct the generation of GC B cells.

The requirement of repeated interactions with APCs is an important feature of T_{FH} differentiation[3], which is presumably connected to the maintenance of the activity of critical transcription factors such as Bcl6[6, 7, 8], Batf[9], STAT3[10, 11, 12], STAT1[10], and Ascl2[13] that support T_{FH} differentiation. Among them, Bcl6 function is absolutely critical. T_{FH} differentiation is completely abrogated in *Bcl6*$^{-/-}$ $CD4^+$ T cells[6, 7, 8] and ectopic *Bcl6* expression in $CD4^+$ T cells leads to augmented T_{FH} differentiation[6, 9]. A number of signaling molecules have been identified that can regulate Bcl6 expression in $CD4^+$ T cells[14]. However, attempts to polarize $CD4^+$ T cells to T_{FH} *in vitro* using IL-6 and IL-21 fail to reproducibly induce Bcl6 and CXCR5 expression. Therefore, there are clear gaps in our understanding of the molecular requirements for Bcl6 induction and the factors that support T_{FH} differentiation[3].

LEF1-1 and TCF-1 (encoded by *Lef1* and *Tcf7*, respectively) are transcription factors that contain a conserved high mobility group (HMG) DNA binding domain. TCF-1 and LEF-1 are known for their essential roles in early T cell development, including T lineage specification and β-selection during the $CD4^-CD8^-$ double negative stage[15, 16]. TCF-1 and LEF-1 critically regulate $CD4^+$ versus $CD8^+$ T cell lineage commitment upon completion of positive selection of $CD4^+CD8^+$ double positive thymocytes[17, 18]. In mature $CD8^+$ T cells, TCF-1 and LEF-1 regulate the generation, maturation and longevity of memory $CD8^+$ T cells in response to viral or bacterial infection[19, 20, 21]. In mature $CD4^+$ T cells, TCF-1 promotes T_H2 differentiation *in vitro* via positive regulation of GATA-3[22]. TCF-1 restrains expression of interleukin 17 (IL-17A) in developing thymocytes and activated $CD4^+$ T cells[23]. In addition, TCF-1 can interact with the transcription factor Foxp3 and appears to oppose Foxp3-mediated gene repression in regulatory $CD4^+$ T cells[24].

Here we looked for undiscovered regulators of early T_{FH} differentiation and found that LEF-1 and TCF-1 are critical transcriptional regulators of T_{FH} differentiation. Using a knock-in reporter system and RNA-seq analysis we found that these transcription factors were highly expressed in T_{FH} cells upon viral or bacterial infections. Genetic deletion of *Lef1*, *Tcf7*, or both factors in $CD4^+$ T cells led to T_{FH} differentiation defects in a dose dependent manner. As a consequence, the magnitude of B cell responses and germinal center reactions was substantially diminished in LEF-1- and TCF-1-deficient mice after infection. Mechanistically, LEF-1 and TCF-1 regulate multiple interacting mechanisms

upstream of Bcl6 to preferentially instruct activated $CD4^+$ T cells to undertake T_{FH} differentiation.

RESULTS

Transcriptional profiles of early T_{FH} cells versus T_H1 cells

Initial $CD4^+$ T cell contact with APCs in the T cell zone can promote expression of key T_{FH} molecules including Bcl6 and CXCR5. By 72 hours into an acute viral infection, the early T_{FH} and T_H1 cells have become fate-committed[25, 26]. Early T_{FH} cells are IL-2Rα^{lo}Bcl6^{hi}Blimp1^{-}CXCR5^{hi} , while early T_H1 cells are IL-2Rα^+ and Tbet^{hi}Bcl6^{-}Blimp1^{hi} in the context of acute viral and bacterial infections[25, 26, 27, 28]. To identify new factors important in the programming of T_{FH} cells we performed gene expression analysis on early T_{FH} and T_H1 cells using RNA-seq. Congenically marked $CD45.1^+$ Blimp1-YFP reporter LCMV-specific TCR transgenic $CD4^+$ T cells (SMARTA) were transferred into B6 host mice given an acute infection with the Armstrong strain of LCMV (LCMV-Arm), and early T_{FH} and T_H1 cells were isolated three days after infection and purified to homogeneity by sorting IL-2Rα^-Blimp1-YFP$^-$ and IL-2Rα^+Blimp1-YFP$^+$ cells, respectively. RNA-seq was performed on the isolated RNA and early T_{FH} and T_H1 transcriptome profiles were obtained (Fig. 1a–b). Analysis revealed that approximately 1,200 genes were upregulated more than 1.5 fold in early T_{FH} cells relative to T_H1 cells, and 1,600 genes were downregulated more than 1.5 fold (Fig. 1b). Early T_{FH} cells expressed many genes that are also preferentially expressed by fully differentiated T_{FH} and GC T_{FH} (*Bcl6*, *Cxcr5*, *Pdcd1*, *Pou2af1* and *Tnfsf8* among others) and had low expression of many genes repressed in fully differentiated T_{FH} and GC T_{FH} (*Prdm1*, *Tbx21*, *IL2ra*, *Gzmb* and *Prf1* among others) (Fig. 1a, b). Thus, major attributes of T_{FH} and T_H1 cells are transcriptionally well defined by day 3 of an acute viral infection.

Lef1 is a transcriptional regulator of T_{FH} differentiation

To further filter the 2,800 gene expression differences between early T_{FH} cells and T_H1 cells, we focused on transcription factors. We then performed an additional set of RNA-seq experiments using i*n vitro* activated $CD4^+$ T cells under T_H1 polarizing conditions (IL-12 + αIL-4 + αTGF-β) or with IL-6 (IL-6 + αIFN-γ+αIL-12). These screening conditions were used because *in vitro* stimulation of $CD4^+$ T cells in the presence of IL-6 resulted in some gene expression changes associated with T_{FH} differentiation (Supplementary Fig. 1a–c. Most notably, *Il21* was robustly induced by IL-6); however, major aspects of T_{FH} biology were not detected in IL-6-stimulated $CD4^+$ T cells, such as CXCR5 protein expression and sustained Bcl6 expression[3, 13, 29, 30] (Supplementary Fig. 1f). This outcome suggested that key transcriptional regulators required for T_{FH} differentiation are not induced under IL-6 conditions *in vitro*. We next performed a comparative analysis of gene expression differences between the *in vivo* generated early T_{FH} and the *in vitro* IL-6 stimulated $CD4^+$ T cells. To reveal critical unidentified early upstream transcriptional regulators of T_{FH} differentiation we focused on genes meeting two conditions: preferential expression by early T_{FH} cells *in vivo* and lack of differential expression after *in vitro* stimulation with IL-6. *Lef1* satisfied these two conditions (Fig. 1b, Supplementary Fig. 1d, g) and was selected for

further analysis in part because LEF-1 is required for the formation of memory $CD8^+$ T cells[20] and there are similarities between T_{FH} and memory $CD8^+$ T cell differentiation[25, 31].

When expressed in SMARTA $CD4^+$ T cells, an shRNAmir expression vector targeting *Lef1* (sh*Lef1*-RV) inhibited expression of both LEF-1 protein isoforms (Fig. 1c). To test whether early T_{FH} differentiation *in vivo* is dependent on LEF-1, SMARTA $CD45.1^+$ $CD4^+$ T cells expressing a control shRNA (sh*Ctrl*) or sh*Lef1*$^+$ SMARTA $CD4^+$ T cells were transferred into B6 mice. Three days after LMCV infection of recipient mice, sh*Lef1*$^+$ SMARTA $CD4^+$ T cells produced approximately half the number of early T_{FH} cells compared to sh*Ctrl*$^+$ SMARTA $CD4^+$ T cells as assessed by flow cytometry using either $Bcl6^+CXCR5^+$ (Fig. 1e) or $IL2R\alpha^-CXCR5^+$ (Fig. 1f) phenotyping. The impact of LEF-1 knock-down was selective to T_{FH} differentiation, as SMARTA $CD4^+$ T cell activation (CD44 upregulation, not shown) and proliferation (Fig. 1d) were comparable between sh*Ctrl*$^+$ and sh*Lef1*$^+$ $CD4^+$ T cells. The reduced T_{FH} differentiation by sh*Lef1*$^+$ $CD4^+$ T cells indicated that LEF-1 may be an important and dose limiting contributor to this process.

Lef1 controls T_{FH} differentiation and germinal center formation

We next examined whether LEF-1 function in $CD4^+$ T cells was important for GC T_{FH} differentiation and germinal center reactions. sh*Lef1*$^+$ or sh*Ctrl*$^+$ SMARTA $CD4^+$ T cells were transferred into B6 mice and analyzed 8 days after acute LCMV infection of the recipient mice. Activation and proliferation of $CD4^+$ T cells were not affected by reduced *Lef1* expression compared to sh*Ctrl* (Fig. 2a), but T_{FH} differentiation of sh*Lef1*$^+$ cells was impaired (Fig. 2b–c). The sh*Lef1*$^+$ T_{FH} defect was less severe than that observed on day 3, potentially due to the fact that sustained gene knock-down in $CD4^+$ T cells *in vivo* is difficult to accomplish under conditions of rapid proliferation. We note that we have observed milder T_{FH} differentiation defects for most shRNAmir-RVs at peak proliferation time points compared to early time points after infection, including shRNAmir against *Bcl6* (data not shown). Nevertheless, sh*Lef1*$^+$ SMARTA $CD4^+$ T cells showed defective differentiation into GC T_{FH}, identified here as $PSGL\text{-}1^{lo}CXCR5^+$ T cells (Fig. 2d) or $Bcl6^+CXCR5^+$ T cells (Fig. 2e), compared to sh*Ctrl*$^+$ SMARTA $CD4^+$ T cells. As a result, the development of GC B cells ($Bcl6^+CD19^+$) was moderately impaired in the presence of sh*Lef1*$^+$ SMARTA $CD4^+$ T cells as compared to sh*Ctrl*$^+$ cells (Fig. 2f). Taken together, reduction of LEF-1 expression in $CD4^+$ T resulted in loss of T_{FH} and GC T_{FH} cells and a proportional loss of GC B cells during an immune response to LCMV.

Ablation of *Lef1* diminishes GC T_{FH} differentiation

We next investigated the role of LEF-1 in T_{FH} differentiation using conditional gene-targeted *Lef1*$^{fl/fl}$ mice. Lineage-specific deletion of *Lef1* in thymocytes with *Cd4*-Cre impairs $CD4^+$ T cell lineage choice and diminishes $CD4^+$ T cell output[18]. To avoid this, we used human CD2 promoter-driven Cre recombinase transgenic mice (h*CD2*-Cre), which achieve gene ablation in mature T cells[32]. Mice were also crossed to the Rosa26-STOP-GFP (*Rosa26*^{GFP}) allele. As marked by GFP expression due to excision of the floxed transcription-translation STOP sequence from *Rosa26*^{GFP} allele, over 70% of splenic $CD4^+$ T cells in h*CD2*-Cre *Rosa26*^{GFP} mice were GFP^+, whereas less than 15% of $CD4^+$ thymocytes were GFP^+ (Supplementary Fig. 2a). We crossed h*CD2*-Cre *Rosa26*^{GFP} to the

Lef1$^{fl/fl}$ strain to generate h*CD2*-Cre *Rosa26*^{GFP}*Lef1*$^{fl/fl}$ mice (called *Lef1*$^{-/-}$ hereafter). Both isoforms of LEF-1 were completed ablated in GFP$^+$ CD4$^+$ T cells from *Lef1*$^{-/-}$ mice (Supplementary Fig. 2b). Late deletion of LEF-1 did not detectably affect thymocyte development or cause aberrant activation of mature T cells (Supplementary Fig. 2d, f, h, i) but reduced total thymic cellularity by approximately 15% and mature CD4$^+$ T cells by approximately 25% (Supplementary Fig. 2e, g). To determine the impact of LEF-1 deficiency in CD4$^+$ T cells on T_{FH} differentiation, we infected *Lef1*$^{-/-}$ mice and littermate controls (h*CD2*-Cre$^-$*Lef1*$^{+/fl}$ or h*CD2*-Cre$^+$*Lef1*$^{+/+}$) with vaccinia virus and assessed the presence of CD44^{hi}CD62L$^-$ activated GFP$^+$ CD4$^+$ splenic T cells on day 8 post infection. The frequency of T_H1 cells (SLAM^{hi}CXCR5$^-$) were similar in *Lef1*$^{-/-}$ mice and littermate control mice, though the absolute numbers of SLAM^{hi}CXCR5$^-$ T_H1 cell were modestly decreased compared to control ($p = 0.51$, Supplementary Fig. 3), consistent with a modestly reduced CD4$^+$ T cell compartment in uninfected *Lef1*$^{-/-}$ mice (Supplementary Fig. 2g). SLAM$^-$CXCR5$^+$ T_{FH} cell numbers were more markedly decreased in the vaccinia virus-immunized *Lef1*$^{-/-}$ mice compared to littermate controls ($p = 0.006$, Fig. 3a). In particular, the number of GC T_{FH} cells were diminished to a much greater extent in *Lef1*$^{-/-}$ mice compared to littermate controls (Bcl6$^+$CXCR5$^+$ and PD-1^{hi}CXCR5$^+$ phenotyping Fig. 3b,c). These data further corroborate a role of LEF-1 in directing T_{FH} differentiation.

TCF-1 expression is retained in T_{FH} but not T_H1 cells

RNA-seq analysis of early T_{FH} and T_H1 cells isolated from B6 mice revealed that *Tcf7* was also strongly expressed by early T_{FH} cells, but *Tcf7* was not induced by *in vitro* stimulation of CD4$^+$ T cells with IL-6 (Fig. 1b, Supplementary Fig. 1e, g). Given that LEF-1 and TCF-1 are related transcription factors, we investigated whether TCF-1 was also an early regulator of T_{FH} differentiation. For this purpose, we generated *Tcf7*-GFP knock-in mice (called *Tcf7*^{GFP} here, Supplementary Fig. 4a). The *Tcf7*-GFP reporter was abundantly expressed in CD4$^+$ and CD8$^+$ T cells and CD4$^+$CD25$^+$ regulatory T cells but was absent in B220$^+$ cells, demonstrating the reporter fidelity (Supplementary Fig. 4b–d). The expression of *Tcf7*-GFP was highest in CD44^{lo}CD62L$^+$ naïve T cells but was low in antigen-experienced T cell subsets such as CD44^{hi}CD62L$^+$ memory-phenotype T cells, and particularly CD44^{hi}CD62L$^-$ effector-phenotype T cells (Supplementary Fig. 4b, c). To analyze TCF-1 expression kinetics in antigen-specific CD4$^+$ T cells we generated *Tcf7*$^{GFP/+}$ SMARTA mice and adoptively transferred naïve CD44^{lo}CD62L$^+$ SMARTA CD45.2$^+$ CD4$^+$ T cells into CD45.1$^+$ congenic recipients. Following LCMV infection, *Tcf7*-GFP expression was greatly diminished in SLAM^{hi} CXCR5$^-$ T_H1 cells by day 8 post-infection compared to naive CD4 T cells, while *Tcf7*-GFP expression was maintained at a high level by most SLAM^{lo}CXCR5$^+$ T_{FH} cells (Fig. 4a).

We next investigated if the retention of TCF-1 expression was associated with the T_{FH} differentiation program in response to other *in vivo* stimuli. Following adoptive transfer of *Tcf7*^{GFP} SMARTA CD4$^+$ T cells, we infected recipient mice with *Listeria monocytogenes* expressing the GP61 epitope of LCMV. In other experiments, we directly infected *Tcf7*$^{GFP/+}$ mice with vaccinia virus, as a second viral infection model. Whereas SLAM^{hi}CXCR5$^-$ T_H1 cells that developed in both systems preferentially downregulated *Tcf7*-GFP expression, SLAM^{lo}CXCR5$^+$ T_{FH} cells generated in response to both the bacterial and viral infections

highly retained *Tcf7*-GFP expression (Supplementary Fig. 4e, f). Considering that TCF-1 is known to be markedly downregulated in effector $CD8^+$ T cells[33], these observations indicate that retention of TCF-1 expression at the effector phase of a T cell response is unique to T_{FH} cells, and further suggest a possible requirement for TCF-1 in T_{FH} differentiation.

Both LEF-1 and TCF-1 are essential for T_{FH} responses

To address the role of TCF-1 in T_{FH} cells, we generated h*CD2*-Cre *Rosa26*^{GFP}*Tcf7*$^{fl/fl}$ mice (called *Tcf7*$^{-/-}$ hereafter), where all isoforms of TCF-1 were ablated from GFP^+ $CD4^+$ T cells (Supplementary Fig. 2c). To investigate the functional redundancy between LEF-1 and TCF-1 we also crossed *Tcf7*$^{-/-}$ with *Lef1*$^{-/-}$ mice to generate *Lef1*$^{-/-}$*Tcf7*$^{-/-}$ mice (h*CD2*-Cre *Rosa26*^{GFP} *Lef1*$^{fl/fl}$*Tcf7*$^{fl/fl}$). Similar to the *Lef1*$^{-/-}$ mice, we did not observe T cell development defects or aberrant activation of mature T cells in *Tcf7*$^{-/-}$ mice or *Lef1*$^{-/-}$*Tcf7*$^{-/-}$ mice (Supplementary Fig. 2). Although a modest reduction in thymic and splenic cellularity was observed in *Tcf7*$^{-/-}$ mice, this was not evident in *Lef1*$^{-/-}$*Tcf7*$^{-/-}$ mice compared to littermate controls (h*CD2*-Cre$^-$*Lef1*$^{+/fl}$*Tcf7*$^{+/fl}$ or h*CD2*-Cre$^+$*Lef1*$^{+/+}$*Tcf7*$^{+/+}$) (Supplementary Fig. 2d, f, h, i). We examined the $CD4^+$ T cell responses of the *Lef1*$^{-/-}$*Tcf7*$^{-/-}$ mice in response to vaccinia virus infection. On day 8 after infection, analysis of $CD44^{hi}CD62L^-$ activated GFP^+ $CD4^+$ T cells revealed that the frequencies and numbers of $SLAM^{lo}CXCR5^+$ T_{FH} cells were diminished in *Tcf7*$^{-/-}$ mice compared to control mice (Fig. 4b), with comparable reduction of GC T_{FH} cells ($Bcl6^+CXCR5^+$ and PD-$1^{hi}CXCR5^+$ phenotyping, Fig. 4c,d). We found stronger defects in *Lef1*$^{-/-}$*Tcf7*$^{-/-}$ mice compared to *Tcf7*$^{-/-}$ mice (Fig. 4b-4d), indicating that both LEF-1 and TCF-1 contribute to regulation of T_{FH} differentiation.

Consistent with the observations above, *Tcf7*$^{-/-}$ and *Lef1*$^{-/-}$*Tcf7*$^{-/-}$ mice exhibited significantly diminished frequency and numbers of $GL7^+Fas^+$ GC B cells compared to control mice (Fig. 4e), with the most severe GC B cell defect in *Lef1*$^{-/-}$*Tcf7*$^{-/-}$ mice (Fig. 4e). The number of $IgD^{lo}CD138^+$ plasma cells was moderately reduced in *Tcf7*$^{-/-}$ mice, but severely compromised in *Lef1*$^{-/-}$*Tcf7*$^{-/-}$ mice (Fig. 4f). As a result, vaccinia virus-specific Ab production was significantly impaired in *Lef1*$^{-/-}$*Tcf7*$^{-/-}$ mice compared to controls (Supplementary Fig. 5). In summary, our data indicate that LEF-1 and TCF-1 play critical roles in T_{FH} differentiation and, consequently, B cell help functions in a $CD4^+$ T cell intrinsic manner.

Ectopic *Lef1* expression augments T_{FH} differentiation

We next tested whether enhanced expression of one of these transcription factors could augment T_{FH} differentiation of antigen-specific $CD4^+$ T cells. Given that LEF-1 and TCF-1 exhibited overlapping activities instructing T_{FH} differentiation, we examined T_{FH} differentiation of $CD4^+$ T cells after ectopic expression of LEF-1. LEF-1 can be expressed as two isoforms in $CD4^+$ T cells due to differential promoter usage (Fig. 1c), with the full-length isoform containing a unique N-terminal β-catenin-binding domain. We used a retrovirus expressing the full-length *Lef1* (*Lef1*-RV^+) and confirmed increased expression of LEF-1 protein in *Lef1*-RV^+ SMARTA $CD45.1^+$ $CD4^+$ T cells by flow cytometry (Fig. 5a) and immunoblot analysis (data not shown). GFP-RV^+ or *Lef1*-RV^+ $CD45.1^+$ SMARTA $CD4^+$ T cells were transferred into B6 mice, which were then infected with LCMV. The

overall activation and proliferation of *Lef1*-RV$^+$ CD4$^+$ T cells was normal compared to GFP-RV$^+$ CD4$^+$ T cells (Fig. 5b and data not shown). Ectopic LEF-1 expression resulted in enhanced T_{FH} development by *Lef1*-RV$^+$ cells compared to GFP-RV$^+$ cells 8 days post-infection (Fig. 5c). Moreover, we found that *Lef1*-RV$^+$ T_H1 cells (SLAM^{hi}CXCR5$^-$) exhibited unexpectedly increased expression of canonical T_{FH} molecules CXCR5 (Fig. 5d) and PD-1 (Fig. 5e) compared to GFP-RV$^+$ cells. Most importantly, GC T_{FH} cells (phenotyped as either PSGL-1^{lo}CXCR5$^+$ or PD-1^{hi}CXCR5$^+$ cells Fig. 5f, g) developed at significantly higher frequencies among *Lef1*-RV$^+$ SMARTA CD4$^+$ T cells compared to GFP-RV$^+$ control cells.

LEF-1 enhances expression of IL-6 receptors and ICOS

To gain insights into how LEF-1 regulates T_{FH} differentiation, we performed RNA-seq on GFP-RV$^+$ or *Lef1*-RV$^+$ CXCR5^{lo} T_H1 and CXCR5^{hi} T_{FH} SMARTA CD4$^+$ T cells. We next used transcriptional signatures of T_{FH} and GC T_{FH} cells (see Methods) and Gene Set Enrichment Analysis (GSEA) to investigate whether these gene expression signatures were enriched in *Lef1*-RV$^+$ T_H1 cells in comparison to control T_H1 cells (GFP-RV$^+$). We found substantial enrichment of the T_{FH} and GC T_{FH} gene signatures (Supplementary Table 1) in T_H1 cells constitutively expressing *Lef1* (NES = 1.21, T_{FH} GSEA; NES = 1.29, GC T_{FH} GSEA, Fig. 6a) compared to control T_H1 cells. Detailed examination revealed that differential expression of *Il6rα*, *Il6st*, *Bcl6*, *Cxcr5*, *Slamf6*, and *Pou2af1* were particularly notable in the *Lef1*-RV$^+$ T_H1 cells compared to GFP-RV$^+$ T_H1 cells (Fig. 6b).

Considering the induction of both IL-6 receptor genes *Il6rα* and *Il6st* in *Lef1*-RV$^+$ T_H1 cells and the fact that IL-6 receptor signaling is one of the earliest signals that instructs T_{FH} cell differentiation[3], we tested whether LEF-1-augmented T_{FH} differentiation may be mediated through enhanced surface expression of IL-6Rα and gp130 (also known as IL-6Rβ, encoded by *Il6st*). We analyzed the expression of IL-6Rα and gp130 on the surface of *Lef1*-RV$^+$ and GFP-RV$^+$ SMARTA CD4$^+$ T cells at day 3 after infection with LCMV, a time when IL-6 receptor signaling is known to be critical for T_{FH} differentiation[10]. Ectopic expression of LEF-1 in *Lef1*-RV$^+$ SMARTA CD4$^+$ T cells resulted in increased expression of IL-6Rα compared to GFP-RV$^+$ SMARTA CD4$^+$ T cells (Fig. 6c). When comparing IL-6Rα expression between naïve CD4$^+$ T cells and activated *Lef1*-RV$^+$ and GFP-RV$^+$ SMARTA CD4$^+$ T cells, LEF-1 overexpression reduced the downregulation of IL-6Rα observed in activated GFP-RV$^+$ CD4$^+$ T cells (Fig. 6c). LEF-1 overexpression had similar effects on gp130, reducing the downregulation of gp130 observed in activated GFP-RV$^+$ CD4$^+$ T cells (Fig. 6d). We then examined the expression of IL-6Rα and gp130 on T_{FH} and T_H1 subpopulations. A modest increase in IL-6Rα expression was observed on T_{FH} cells, whereas *Lef1*-RV$^+$ T_H1 cells expressed >150% more IL-6Rα compared to GFP-RV$^+$ T_H1 cells (Fig. 6e). While the expression of gp130 was only moderately increased in total *Lef1*-RV$^+$ SMARTA CD4$^+$ T cells compared to GFP-RV$^+$ SMARTA CD4$^+$ T cells (Fig. 6d), gp130 was preferentially upregulated on *Lef1*-RV$^+$ T_H1 cells compared to GFP-RV$^+$ T_H1 cells (Fig. 6f).

RNA-seq also revealed that *Icos* expression was upregulated on *Lef1*-RV$^+$ T_H1 cells compared to GFP-RV$^+$ T_H1 cells (Fig. 6b). Because ICOS plays essential roles during both

early and late stages of T_{FH} differentiation[26], we further examined ICOS expression. ICOS protein was increased in *Lef1*-RV$^+$ T cells compared to GFP-RV$^+$ cells (Fig. 6g), and its upregulation occurred predominantly on *Lef1*-RV$^+$ T_H1 cells (Fig. 6h), to levels comparable to GFP-RV$^+$ T_{FH} cells. These observations indicate that LEF-1 functions to help CD4$^+$ T cells retain surface expression of IL-6 receptors and upregulate ICOS expression to enhance responsiveness of activated CD4$^+$ T cells to IL-6 and ICOS-L signals, two essential signals for early T_{FH} differentiation.

We then asked whether overexpression of LEF-1 could rescue T_{FH} differentiation in the absence of Bcl6. *Cd4*-Cre *Bcl6*$^{fl/fl}$ CD4$^+$ T cells fail to differentiate into T_{FH} cells during acute viral infections or protein immunizations[34]. *Lef1*-RV$^+$ or GFP-RV$^+$ *Cd4*-Cre *Bcl6*$^{fl/fl}$ SMARTA CD4$^+$ T cells transferred into B6 mice failed to differentiate into T_{FH} cells *in vivo* at day 8 after LCMV infection of the recipient mice (Supplementary Fig. 6). These results indicate that LEF-1-mediated regulation of IL-6 receptor complex and ICOS expression act upstream of Bcl6 expression early in T_{FH} differentiation.

Lef1$^{-/-}$ *Tcf7*$^{-/-}$ GC T_{FH} cells have extensive gene regulation defects

We further assessed the requirements of LEF-1 and TCF-1 for expression of key T_{FH} molecules by transcriptomic analysis of *Lef1*$^{-/-}$*Tcf7*$^{-/-}$ GC T_{FH} cells. RNA-seq was performed using total RNA extracted from GC T_{FH} cells (sorted as PD-1^{hi}CXCR5$^+$ of CD44^{hi}CD62L^{lo}GFP$^+$CD4$^+$ T cells) isolated from *Lef1*$^{-/-}$*Tcf7*$^{-/-}$ and control mice (h*CD2*-Cre$^-$*Lef1*$^{+/fl}$*Tcf7*$^{+/fl}$ or h*CD2*-Cre$^+$*Lef1*$^{+/+}$*Tcf7*$^{+/+}$) on day 8 after vaccinia virus infection. 306 genes were downregulated and 668 genes upregulated in *Lef1*$^{-/-}$*Tcf7*$^{-/-}$ GC T_{FH} cells in comparison to control GC T_{FH} cells (FDR < 0.01 and fold change ≥ 1.5, Fig. 7a). In line with the enhanced *Il6st* and *Icos* expression induced by overexpression of LEF-1, *Lef1*$^{-/-}$*Tcf7*$^{-/-}$ GC T_{FH} cells had greatly reduced *Il6st* and *Icos* transcripts compared to control cells (Fig. 7b). Flow cytometry showed decreased expression of gp130 and ICOS protein on *Lef1*$^{-/-}$*Tcf7*$^{-/-}$ CXCR5$^+$ T_{FH} cells compared to T_{FH} cells from controls (Fig. 7c and 7d). Although the decrease of *Il6ra* mRNA in *Lef1*$^{-/-}$*Tcf7*$^{-/-}$ GC T_{FH} cells did not reach statistical significance in the transcriptomic analysis, IL-6Rα protein expression was consistently reduced on *Lef1*$^{-/-}$*Tcf7*$^{-/-}$ CXCR5$^+$ T_{FH} cells compared to T_{FH} cells from control mice ($P < 0.001$, Fig. 7e). These observations indicate essential and overlapping roles of both LEF-1 and TCF-1 in supporting IL-6 receptor and ICOS expression during T_{FH} differentiation.

The amount of *Bcl6* transcripts was diminished in PD-1^{hi}CXCR5$^+$ GC T_{FH} cells from *Lef1*$^{-/-}$*Tcf7*$^{-/-}$ mice compared to those from control mice (Fig. 7b), while the expression of *Prdm1*, which encodes the transcription factor Blimp1, was substantially elevated in *Lef1*$^{-/-}$*Tcf7*$^{-/-}$ GC T_{FH} cells (Fig. 7b). Bcl6 and Blimp1 are known to have mutually antagonistic roles during differentiation of T_{FH} cells[6]. Blimp1 directly inhibits Bcl6 expression and is a potent inhibitor of T_{FH} differentiation[6, 28, 30]. We validated the increased expression of *Prdm1* in *Lef1*$^{-/-}$*Tcf7*$^{-/-}$ PD-1^{hi}CXCR5$^+$ GC T_{FH} by qPCR (Fig. 7f). This increase was specific to GC T_{FH} (PD-1^{hi}CXCR5$^+$) and T_{FH} (PD-1^{lo}CXCR5$^+$) cells because T_H1 cells (CXCR5$^-$) from both *Lef1*$^{-/-}$*Tcf7*$^{-/-}$ and control mice expressed comparable levels of *Prdm1* (Fig. 7f). The transcription factor Ascl2 was shown to be important in T_{FH}

differentiation[13]. *Ascl2* expression was reduced in *Lef1*$^{-/-}$*Tcf7*$^{-/-}$ GC T_{FH} cells, but the reduction was less pronounced in PD-1^{lo}CXCR5^{+} T_{FH} cells compared to controls (Fig. 7f). *Rorc* (encoding RORγt) and *Il17a* were virtually absent in control GC T_{FH} cells, but these genes were expressed in *Lef1*$^{-/-}$*Tcf7*$^{-/-}$ GC T_{FH} cells (Fig. 7b). Although Th17 gene expression is not normally observed in vaccinia virus infection, these observations are in line with the known role of TCF-1 in restraining Th17 differentiation[23] and indicate that LEF-1 and TCF-1 could suppress alternative T_H cell fates during T_{FH} differentiation, perhaps in conjunction with Bcl6, which is also known to suppress alternative cell fates[3]. Other transcriptional changes observed in *Lef1*$^{-/-}$*Tcf7*$^{-/-}$ GC T_{FH} cells compared to control GC T_{FH} cells included the differential expression of POU family transcription factors (decreased expression of *Pou2af1* and *Pou6f1*, and increased expression of *Pou3f1* and *Pou5f1*) and key molecules in the Notch pathway (decreased expression of *Hes5* and *Psen2*, and increased expression of *Rbpj*). The role of these factors in T_{FH} cells remains to be investigated. Overall, these observations suggest that LEF-1 and TCF-1 contribute to regulation of many genes in activated, antigen-specific CD4^{+} T cells *in vivo*, including the positive regulation of Bcl6 and repression of Blimp1 to induce T_{FH} differentiation.

TCF-1 binds directly to key T_{FH}-associated gene loci

We used chromatin immunoprecipitation (ChIP) to assess if LEF-1 and TCF-1 directly regulate the differentially expressed genes identified above. Both TCF-1 and LEF-1 have a highly homologous HMG DNA binding domain which recognizes the same DNA consensus motif. Because TCF-1 ChIP reagents are of substantially higher quality than currently available LEF-1 reagents, we focused on identifying TCF-1 bound genes in T_{FH} cells. Because most T_{FH} cells retained TCF-1 expression similar to naïve CD4^{+} T cells (Fig. 4a), we used our TCF-1 ChIP-seq data from naïve wild-type CD4^{+} T cells (unpublished) as a reference for selection of potential TCF-1 DNA binding sites. TCF-1 enrichment was observed at the transcription start site (TSS) of *IL6st*, the TSS of *Bcl6*, a −2.8kb region upstream of *Bcl6* TSS and intron 3 of *Prdm1* in naïve CD4^{+} T cells, but was not associated with the *Il6ra* and *Ascl2* genes (Supplementary Fig. 7a). We then performed TCF-1 ChIP using wild-type and *Tcf7*$^{-/-}$ naïve CD4^{+} T cells to ensure binding specificity. As a positive control, TCF-1 bound to the TSS of *Axin2*, a well characterized TCF-1 responsive gene[15], in wild-type naïve CD4^{+} T cells, and this was completely abrogated in *Tcf7*$^{-/-}$ naïve CD4^{+} T cells (Fig. 8a). In addition, TCF-1 binding to *Axin2* was enriched in T_{FH} cells (CXCR5^{+}) over T_H1 cells (CXCR5^{-}) from B6 mice infected with vaccinia virus (Fig. 8a), consistent with increased expression of TCF-1 protein in T_{FH} cells. TCF-1 bound to the *Il6st* gene in wild-type naïve CD4^{+} T cells (Fig. 8b, right), and this was also enriched in T_{FH} cells (Fig. 8b). Although TCF-1 did not bind the *Il6ra* gene in wild-type naïve CD4^{+} T cells, it was recruited to the *Il6ra* TSS in wild-type T_{FH} cells (Fig. 8b, left), suggesting TCF-1 recruitment to this site is part of the T_{FH} differentiation program. Compared to naïve CD4^{+} T cells, TCF-1 did not exhibit enriched binding at *Il6st* or *Il6ra* locus in wild-type T_H1 cells, in line with diminished expression of both IL-6Rα and gp130 in T_H1 cells (Fig. 7c, e). TCF-1 binding to the transcription start site of *Icos* was not detected (Supplementary Fig. 7b) These data suggest that TCF-1 directly regulates the induction of IL-6 receptor chains to sustain IL-6 receptor complex expression by activated CD4^{+} T cells *in vivo*, allowing for T_{FH} differentiation (Supplementary Fig. 8).

We next examined ChIP association between TCF-1 and key transcription factor genes for T_{FH} differentiation. TCF-1 bound to intron 3 of the *Prdm1* gene, the major regulatory site of *Prdm1* expression[35], in both naïve $CD4^+$ T cells and $CXCR5^+$ T_{FH} cells (Fig. 8d), suggesting a direct involvement of TCF-1 and its homologue LEF-1 in Blimp1 suppression in T_{FH} cells. Given that *Prdm1* is not expressed by naïve $CD4^+$ T cells, binding of TCF-1 at this site suggests that TCF-1 may antagonize *Prdm1* expression upon T cell activation. In addition, we observed specific binding of TCF-1 to the TSS of *Bcl6* and an upstream regulatory region of *Bcl6* in naive $CD4^+$ T cells (Fig. 8c) and this binding pattern was maintained in T_{FH} cells (Fig. 8c). Robust enrichment of TCF-1 was observed in the *Prdm1*, *Bcl6*, *Il6ra*, and *Il6st* gene loci in wild-type T_{FH} cells compared to $Tcf7^{-/-}$ T_{FH} cells (Supplementary Fig. 7b). We did not observe enriched TCF-1 binding in the *Ascl2* TSS (Fig. 8c–d), albeit we could not exclude the possibility that *Ascl2* is regulated by LEF-1 and TCF-1 through more distal regulatory regions. TCF-1 binding to the *Bcl6* upstream region and *Prdm1* intron was abrogated in T_H1 cells as compared to T_{FH} (Fig. 8d), in line with the greatly reduced expression of TCF-1 in T_H1 cells. These observations suggest that downregulation of TCF-1 in T_H1 cells is important for upregulation of Blimp1 and Blimp1-mediated repression of Bcl6 in T_H1 cells, while retention of TCF-1 in early T_{FH} cells ensures proper upregulation of Bcl6 and subsequent suppression of Blimp1 during T_{FH} differentiation (Supplementary Fig. 8).

DISCUSSION

T_{FH} differentiation can be initiated at an early time point during T cell activation, but the regulators of this important decision process are still being defined. Here we initiated an investigation to identify novel pathways in T_{FH} differentiation by characterizing genes differentially expressed in early T_{FH} *in vivo* but not modulated by supplementing IL-6 *in vitro*. We show that the pair of transcription factors LEF-1 and TCF-1 influence T_{FH} differentiation by regulating circuits upstream of Bcl6. We found that LEF-1 and TCF-1 coordinate T_{FH} differentiation by two general mechanisms. First, they establish the responsiveness of naïve $CD4^+$ T cells to T_{FH} signals by promoting expression of IL-6 receptor chains and binding to *Prdm1* and *Bcl6*. Second, they promote early T_{FH} differentiation of activated $CD4^+$ T cells via multipronged activities sustaining expression of IL-6Rα and gp130, enhancing ICOS expression and promoting expression of Bcl6 while inhibiting Blimp1 expression.

IL-6 is a critical early regulator of T_{FH} differentiation, as $Il6^{-/-}$ mice fail to have any T_{FH} cell differentiation during the DC priming phase of an acute antiviral immune response[10]. In mice whose DCs constitutively overexpress IL-6, the major phenotype observed is a dramatic increase in T_{FH} cell and germinal centers[36]. Therefore, regulation of IL-6 receptor expression on naive $CD4^+$ T cells and early activated $CD4^+$ T cells is a clear mechanism by which LEF-1 and TCF-1 will influence T_{FH} differentiation.

Bcl6 is essential for T_{FH} differentiation, while Blimp1 is a powerful antagonist of T_{FH} differentiation. Our observations that expression of LEF-1 results in aberrant expression of Bcl6 in T_H1 cells, Blimp1 expression is aberrantly upregulated in $Lef1^{-/-}Tcf7^{-/-}$ GC T_{FH} cells, and both *Bcl6* and *Prdm1* are directly bound TCF-1 targets indicate that LEF-1 and

TCF-1 likely dually regulate both of these critical transcription factors. While we cannot rule out the possibility that the de-repression of *Prdm1* results from reduced Bcl6 expression in *Lef1*$^{-/-}$*Tcf7*$^{-/-}$ T_{FH} and GC T_{FH} cells, we speculate that LEF-1 and TCF-1 directly repress *Prdm1* expression. LEF-1 and TCF-1 are known to positively and negatively regulate gene expression, depending on the interacting factors. For examples, both proteins can interact with β-catenin coactivator and TLE corepressors, and LEF-1 and TCF-1 repress *Cd4* in $CD8^+$ T cells[18]. Future analysis of molecular mechanisms by which LEF-1 and TCF-1 regulate *Prdm1* and *Bcl6* genes will be important, as will analysis of how LEF-1 and TCF-1 interact with other regulators of *Bcl6* and *Prdm1*, such as STAT1, STAT3, STAT5, Foxo1, and Klf2[3, 10, 11, 28, 37, 38]. Nevertheless, our data provide proof that LEF-1 and TCF-1 regulate the balance between Bcl6 and Blimp1 expression.

ICOS expression was selectively impaired on *Lef1*$^{-/-}$*Tcf7*$^{-/-}$ T_{FH} cells, and ICOS expression was enhanced on *Lef1*-RV^+ cells. In multiple models, moderate ICOS changes have been observed to enhance T_{FH} differentiation[38, 39, 40, 41] or function[42]. ICOS appears not to be a direct target of LEF-1 and TCF-1, though distal *cis*-elements were not explored. Alternatively, ICOS may be indirectly regulated by LEF-1 and TCF-1. Future studies will further elucidate LEF-1 and TCF-1 signaling axes modulating ICOS expression. Overall, the combined influence of LEF-1 and TCF-1 on IL-6Rα, gp130, Bcl6, Blimp1, and ICOS makes a dense network of interactions that create a strong pro-T_{FH} signaling environment in a cell sustaining LEF-1 and/or TCF-1 expression.

LEF-1 and TCF-1 functions likely continue to be important in fully differentiated T_{FH} and GC T_{FH} cells. LEF-1 and TCF-1 both continue to be expressed in GC T_{FH} cells. Bcl6 expression is essential in GC T_{FH} cells[3] and continued regulation of both *Bcl6* and *Prdm1* are central aspects of GC T_{FH} biology. ICOS is also a major regulator of GC T_{FH} biology[26, 40]. IL-6 receptor signaling is not usually essential in GC T_{FH} cells due to compensatory capabilities of IL-21 or IL-27 at later time points[29, 43, 44]. Nevertheless, IL-6 receptor likely plays a major role in sustaining GC T_{FH} under normal physiological conditions. IL-6 is required for sustaining T_{FH} and GC responses in chronic LCMV infection in mice[45], and IL-6 is positively associated with T_{FH} cells and GCs in SIV^+ macaques[46].

The activities of LEF-1 and TCF-1 appear to pre-program the responsiveness of a given naive $CD4^+$ T cell to T_{FH} signals, prior to any exposure of the cell to antigen. Therefore, we speculate that transient or sustained inflammatory or pathogenic conditions that alter LEF-1 or TCF-1 expression in naive T cells may have a global impact altering the capacity of naive $CD4^+$ T cells to respond to T_{FH} induction signals in the presence of pathogens or autoimmunity triggers. Ultimately, it will be useful to determine how homeostatic signals act in concert with LEF-1 and TCF-1 to modulate the expression or poised status of T_{FH}-associated genes in naïve $CD4^+$ T cells to properly orchestrate the development progression from naive cell to T_{FH} or non-T_{FH} cell fates.

LEF-1 and TCF-1 are highly expressed in resting naive $CD4^+$ and $CD8^+$ T cells, but TCF-1 and LEF-1 are downregulated in effector $CD8^+$ T cells and T_H1 cells, suggesting *Lef1* and *Tcf7* are regulated by T cell activation. TCR dwell time influences T_{FH} versus non-T_{FH}

differentiation in a TCR signal strength intrinsic manner[47]. We speculate these processes may be interrelated.

In conclusion, our study discovers novel roles for LEF-1 and TCF-1 in T_{FH} differentiation. Thus, a better understanding of the signals regulating LEF-1 and TCF-1 and their downstream targets in activated $CD4^+$ T cells will have implications for understanding how to enhance T_{FH} differentiation, as well as for understanding non-T_{FH} $CD4^+$ T cell differentiation processes.

METHODS

Mice and viral infections

C57BL/6J (B6), B6.SJL, *Cd4*-Cre, and *Rosa26*^{GFP} mice were purchased from the Jackson Laboratory. Mouse strains described below were obtained from in-house breeders of either LJI or University of Iowa animal facility. SMARTA (LCMV gp66-77-IA^b specific) TCR transgenic mice[48], *Tcf7*$^{fl/fl}$ and *Lef1*$^{fl/fl}$ mice were described[16, 18]. *Bcl6*$^{fl/fl}$ mice and h*CD2*-Cre mice were from Drs. Toshitada Takemori[49] and Paul Love[32], respectively. Blimp1-YFP BAC transgenic mice were crossed to the SMARTA strain to generate Blimp1-YFP SMARTA mice[26]. *Tcf7*-GFP reporter mice were generated in house, and detailed targeting strategy and characterization will be published elsewhere (manuscript in review). All animals were analyzed at 6–12 weeks of age, and both genders included without randomization or “blinding”. All mouse experiments were performed under protocols approved by the Institutional Animal Use and Care Committees of LJI and the University of Iowa. For acute viral infection, $2.5 – 5.0 \times 10^5$ plaque-forming units (PFU) and 2.5×10^5 PFU was used for LCMV Armstrong (LCMV-Arm) and vaccinia virus, respectively. Virus was prepared in plain DMEM and injected intraperitoneally or intravenously.

Flow cytometry

Single cell suspension was prepared from the spleen of mice infected with LCMV or vaccinia virus, and surface-stained as previously described[16, 26]. The fluorochrome-conjugated antibodies and their clone numbers are CD4 (RM4-5), CD44 (IM7), CD62L (MEL-14), PD-1 (J43), IL-6Rα (D7715A7), gp130 (KGP130), ICOS (C398.4A), Fas (15A7), GL7 (GL7), IgD (11–26), CD138 (281-2), Bcl6 (K112-91), and all were from eBiosciences. SLAM (TC15-12F12.2) was from BioLegend. PSGL-1 (2PH1) was from BD Biosciences. For detection of CXCR5, a two-step[26] or three-step[6] staining protocol was used with biotinylated anti-CXCR5 or unconjugated anti-CXCR5 Abs, respectively (2G8 from BD Biosciences). For intracellular detection of Bcl6, the surface-stained cells were fixed and permeabilized with the Foxp3/transcription factor staining buffer (eBiosciences), followed by incubation with fluorochrome-conjugated Bcl6 antibody. Data were collected on LSRII and FACSVerse (BD Biosciences) and analyzed with FlowJo software (TreeStar).

Immunoblot

For analysis of knockdown of LEF-1 or targeted deletion of TCF-1 and LEF-1, sh*Ctrl* and sh*Lef1* SMARTA cells or $CD4^+$ and $CD8^+$ T cells (5×10^5 each) were sorted, and denatured in SDS Loading Buffer at 100°C for 5 minutes. Cell lysates were probed with anti-TCF-1

(C46C7; Cell Signaling Technology), anti-LEF-1 (C18A7 and C12A5; Cell Signaling Technology) or anti-β-actin (loading control; I-19; Santa Cruz Biotechnology).

Retroviral transductions

Naïve SMARTA CD4$^+$ T cells were purified by negative selection using either magnetic beads (Miltenyi Biotec) or EasySep kit (STEMCELL), and resuspended in D-10 [DMEM + 10% FCS (fetal calf serum) + 2 mM GlutaMax (Life Technologies) + 100 U/ml Penicillin/Streptomycin (Life Technologies) + 50 μM β-mercaptoethanol] with 2 ng/ml hIL-7 or 10 ng/ml hIL-2 (Peprotech). 2 × 10^6 SMARTA cells were seeded in 24-well plates coated with 8 μg/ml anti-CD3 (clone 17A2, BioXcell) and anti-CD28 (clone 37.51, BioXcell). Retroviral soups were given at 24 and 36 hours after stimulation. After 72 hours *in vitro* stimulation, SMARTA cells were transferred into 6-well plates in D-10 with 10 ng/ml hIL-2 for two days. One day prior to cell sorting reporter expressing cells (FACSAria, BD Biosciences) for transfer, culture media was replaced with D-10 with 2 ng/ml hIL-7. Detailed information is described elsewhere[50].

Cell sorting

All the cell sorting was done on a FACSAria (BD Biosciences). For RNA-seq analyses, early T_{FH} (IL-2Rα$^-$Blimp1-YFP$^-$) or early T_H1 (IL-2Rα$^+$Blimp1-YFP$^+$) SMARTA cells, or CXCR5$^-$ (T_H1), PD1^{lo}CXCR5$^+$ (T_{FH}), and PD1^{hi}CXCR5$^+$ (GC T_{FH}) subsets among activated GFP$^+$CD4$^+$ splenic T cells of *Lef1*$^{-/-}$*Tcf7*$^{-/-}$ or control mice were sorted on day 3 after LCMV infection or on day 8 after vaccinia virus infection, respectively. GFP-RV$^+$ or *Lef1*-RV$^+$ SMARTA cells were sorted as SLAM^{hi}CXCR5^{lo} (T_H1) or SLAM^{lo}CXCR5^{hi} (T_{FH}) cells on day 4 after LCMV infection. For ChIP analysis, CXCR5$^-$ (T_H1) and CXCR5$^+$ (T_{FH}) cells were sorted from activated CD4$^+$ splenic T cells on day 8 after vaccinia virus infection. Also, CD44^{lo}CD62L^{hi} naïve CD4$^+$ T cells were sorted from WT or *Tcf7*$^{-/-}$ (*Cd4*-Cre*Tcf7*$^{fl/fl}$).

Retrovirus production and cell transfers

Murine *Lef1* cDNA (clone ID 6401514, Open Biosystems) was cloned into expressing retroviral vector (pMIG-GFP). *Lef1* shRNA sequence (Transomic) was cloned into pLMPd-Ametrine vector, as reported[26, 31]. Virions were obtained from the Plat-E cells as described[50]. Briefly, culture supernatants were collected 24 and 48 hours after transfection, filtered through 0.45 μm syringe filter, and saved at 4°C until used for transductions.

Naïve or retrovirally transduced SMARTA cells were transferred into mice intravenously via retro-orbital sinus. When using transduced SMARTA cells, 100% of transferred cells were transduced (Ametrine$^+$CD45.1$^+$). Cell transfer numbers are 4–5 × 10^5, 2 × 10^5, and 5 × 10^3 SMARTA cells were day 3, 4, and 8 experiments, respectively.

In vitro activation of CD4$^+$ T cells

Naïve SMARTA cells were negatively isolated by using CD4$^+$ T cell isolation kit (Miltenyi or StemCell). 2 × 10^6 SMARTA cells were seeded on 24 well plates coated with 8 μg/mL αCD3 (clone 17A2, BioXcell) and αCD28 (clone 37.51, BioXcell). For $T_H1$polarization, Smarta cells were given with 20 μg/mL of αIL-4 (clone 11B11, BioXcell) and αTGF-β

(clone 1D11, BioXcell) and 20 ng/mL of rmIL-12 (Peprotech). For IL-6 condition, 10 μg/mL of αIFN-γ (clone XMG1.2, BioXcell) and αIL-12 (clone R1-5D9, BioXcell) and 20 ng/mL of rmIL-6 (Peprotech) were added in culture media.

Quantitative RT-PCR

Total RNA from the sorted cells was extracted, reverse-transcribed, and quantitative PCR were performed as described[16].

RNA-Seq and transcriptome analysis (Xue Group)

Total RNA was extracted from the sorted PD-1^{+}CXCR5^{+} cells from *Tcf7*$^{-/-}$*Lef1*$^{-/-}$ or control mice, and two biological replicates were obtained for each genotype. cDNA synthesis and amplification were performed using SMARTer Ultra Low Input RNA Kit (Clontech) starting with 10 ng of total RNA per sample following manufacturer's instructions. cDNA was fragmented with Q800R sonicator (Qsonica) and used as input for NEBNext Ultra DNA Library Preparation Kit (NEB). Libraries were sequenced on Illumina's HiSeq2000 in single read mode with the read length of 50 nucleotides producing 60–70 million reads per sample. Sequence data in fastq format were generated using CASAVA 1.8.2 processing pipeline from Illumina.

The sequencing quality of RNA-Seq libraries was assessed by FastQC (http://www.bioinformatics.babraham.ac.uk/projects/fastqc/, v0.10.1). Because of biased GC content in the 5' end, the first 12 bases of each read in all 4 samples were trimmed off. RNA-Seq data reproducibility was evaluated by computing Pearson's correlation of FPKM values for all genes between biological replicates. The Pearson's correlation coefficient between the two biological replicates was 0.937 for the control samples and 0.986 for the *Tcf7*$^{-/-}$ *Lef1*$^{-/-}$ samples, indicating strong reproducibility.

The RNA-Seq libraries were then processed by RSEM (v1.2.19) to estimate expression levels of all genes. The expression level of a gene is expressed as a gene-level FPKM (Fragments Per Kilobase of transcripts per Million mapped reads) value. EBSeq (v1.5.4), as an integral component of RSEM package, was used to identify differentially expressed genes. UCSC genes for mouse mm9 from iGenome (http://support.illumina.com/sequencing/sequencing_software/igenome.html) were used for gene annotation. The RNA-seq data are deposited at the Gene Expression Omnibus under accession number GSE66781.

RNA-Seq and transcriptome analysis (Crotty Group)

Total RNA was extracted from cells stored in Trizol using the miRNeasy Mini Kit (Qiagen 217004). [1] For RNA-seq analysis for early T_{FH} and T_H1 cells: poly(A) RNA was isolated using the Poly(A) Purist MAG kit (Ambion AM1922) from 200 ng total RNA of each sample. Resulting poly(A) RNA was then fragmented and prepared, according to the manufacturer's instructions (ABI 4452437 Rev B), into barcoded, strand-specific libraries using The SOLiD Total RNA-Seq Kit (ABI 4445374). Following library preparation, 15 ng of each library was converted into SOLiD Wildfire compatible fragments using the 5500 W Conversion Primer Kit (Life Technologies) and 5 rounds of PCR. Libraries were then pooled at equimolar concentrations using Quant-iT PicoGreen dsDNA Assay Kit (Life

Technologies) and sequenced on a Life Technologies 5500XL W Genetic Analyzer. SOLiD 5500-2 sequencing outcomes were converted from color space to nucleotide space by using Galaxy solid2fastq script. [2] For RNA-seq analysis for GFP-RV$^+$ or *Lef1*-RV$^+$ SMARTA cells obtained 4 days after LCMV infection: 500 ng of each sample's total RNA was then prepared into mRNA libraries, according to manufacturer's instructions (Illumina, RS-122-2103). The resulting libraries were deep sequenced on the Illumina 2500 in Rapid Run Mode, using single-end reads with lengths of 50 nucleotides (> 24 million reads per condition). The single-end reads that passed Illumina filters were filtered for reads aligning to tRNA, rRNA, adapter sequences, and spike-in controls.

The reads were then aligned to UCSC mm9 reference genome using TopHat (v 1.4.1). DUST scores were calculated with PRINSEQ Lite (v 0.20.3) and low-complexity reads (DUST > 4) were removed from the BAM files. The alignment results were parsed via the SAMtools to generate SAM files. Read counts to each genomic feature were obtained with the htseq-count program (v 0.6.0) using the "union" option. After removing absent features (zero counts in all samples), the raw counts were then imported to R/Bioconductor package DESeq2 to identify differentially expressed genes among samples. DESeq2 normalizes counts by dividing each column of the count table (samples) by the size factor of this column. The size factor is calculated by dividing the samples by geometric means of the genes. This brings the count values to a common scale suitable for comparison. P-values for differential expression are calculated using binomial test for differences between the base means of two conditions. These p-values are then adjusted for multiple test correction using Benjamini Hochberg algorithm to control the false discovery rate. We considered genes differentially expressed between two groups of samples when the DESeq2 analysis resulted in an adjusted P-value of <0.05 and the fold-change in gene expression was 1.5-fold. Cluster analyses including principal component analysis (PCA) and hierarchical clustering were performed using standard algorithms and metrics. Hierarchical clustering was performed using complete linkage with Euclidean metric. RNA-seq data are deposited at the Gene Expression Omnibus under accession number GSE67336.

Heatmaps

Heatmaps were generated with normalized data of RNA-seq analyses for early T_{FH}/T_H1 cells and for GFP-RV$^+$/Lef1-RV$^+$ T_{FH}/T_H1 cells. Microarray analysis used published T_H1, T_{FH} and GC T_{FH} cell sets (GSE21380, ref. [51]) using the GenePattern software suite (genepattern.broadinstitute.org).

GSEA analysis

GSEA analysis was performed using the GSEA software from the Broad Institute. T_{FH} and GC T_{FH} gene sets were generated in-house with genes that were expressed in T_{FH} (PD1^{lo}CXCR5$^+$) and GC T_{FH} (PD1^{hi}CXCR5$^+$) by more than 2-fold in comparison to T_H1 (PD1$^-$CXCR5$^-$) cells, respectively (data obtained from GSE21380). Enrichment of genes, which were upregulated in *Lef1*-RV$^+$ Th1 cells in comparison to GFP-RV$^+$ T_H1 cells by more than 1.2-fold, was then ranked by the Diff_of_Classes.

Chromatin immunoprecipitation (ChIP)

Sorted $CD4^+$ T cells were cross-linked with 1% formaldehyde in medium for 5 minutes, processed using truChIP Chromatin Shearing Reagent Kit (Covaris), and sonicated for 5 minutes on Covaris S2 ultrasonicator. The sheared chromatin was immunoprecipitated with anti-TCF-1 (C46C7, Cell Signaling Technologies) or control rabbit IgG and washed as previously described. The immunoprecipitated DNA segments were used for PCR quantification. For calculation of enriched TCF-1 binding in a given cell type, each TCF-1 ChIP sample was first normalized to corresponding IgG ChIP sample, and the signal at a target region was then normalized to that at the *Hprt* promoter region.

Statistical analysis

Data sets were analyzed with the Student's *t*-test with a two-tailed distribution assuming equal sample variance.

Supplementary Material

Refer to Web version on PubMed Central for supplementary material.

ACKNOWLEDGEMENTS

We thank J. Yang for helping *ex vivo* screening of target genes obtained from RNA-seq analysis for early T_{FH} and T_H1 cells and Z. Fu for generous help in performing GSEA analysis and for the generation of heatmap. We also thank LJI Flow Cytometry Flow Cytometry Core Facility (C. Kim, K.V. Gunst, and L. Nosworthy) and the University of Iowa Flow Cytometry Core facility (J. Fishbaugh, H. Vignes and G. Rasmussen) for cell sorting. We thank I. Antoshechkin (Millard and Muriel Jacobs Genetics and Genomics Laboratory at the Caltech) for $Tcf7^{-/-}Lef1^{-/-}$ RNA-seq, and J. T. Harty for providing *vaccinia* virus to the Xue laboratory. This study is supported by grants from the American Cancer Society (RSG-11-161-01-MPC to H.-H.X.), and the NIH (AI105351, AI112579, AI115149, and AI119160 to H.-H.X., AI113806 to W.P., and AI109976, AI063107, and AI072543 to S.C.). J.A.G is supported in part by a Pre-doctoral Immunology Training Grant AI007485. The content is solely the responsibility of the authors and does not necessarily represent the official views of the US National Institutes of Health.

REFERENCES

1. Crotty S. A brief history of T cell help to B cells. Nature reviews Immunology. 2015; 15(3):185–189.
2. Ueno H, Banchereau J, Vinuesa CG. Pathophysiology of T follicular helper cells in humans and mice. Nature Immunology. 2015; 16(2):142–152. [PubMed: 25594465]
3. Crotty S. T follicular helper cell differentiation, function, and roles in disease. Immunity. 2014; 41(4):529–542. [PubMed: 25367570]
4. Shlomchik MJ, Weisel F. Germinal center selection and the development of memory B and plasma cells. Immunological reviews. 2012; 247(1):52–63. [PubMed: 22500831]
5. Victora GD, Nussenzweig MC. Germinal centers. Annu Rev Immunol. 2012; 30:429–457. [PubMed: 22224772]
6. Johnston RJ, Poholek AC, Ditoro D, Yusuf I, Eto D, Barnett B, et al. Bcl6 and Blimp-1 are reciprocal and antagonistic regulators of T follicular helper cell differentiation. Science. 2009; 325(5943):1006–1010. [PubMed: 19608860]
7. Nurieva RI, Chung Y, Martinez GJ, Yang XO, Tanaka S, Matskevitch TD, et al. Bcl6 mediates the development of T follicular helper cells. Science. 2009; 325(5943):1001–1005. [PubMed: 19628815]
8. Yu D, Rao S, Tsai LM, Lee SK, He Y, Sutcliffe EL, et al. The transcriptional repressor Bcl-6 directs T follicular helper cell lineage commitment. Immunity. 2009; 31(3):457–468. [PubMed: 19631565]

9. Ise W, Kohyama M, Schraml BU, Zhang T, Schwer B, Basu U, et al. The transcription factor BATF controls the global regulators of class-switch recombination in both B cells and T cells. Nature Immunology. 2011; 12(6):536–543. [PubMed: 21572431]
10. Choi YS, Eto D, Yang JA, Lao C, Crotty S. Cutting Edge: STAT1 Is Required for IL-6-Mediated Bcl6 Induction for Early Follicular Helper Cell Differentiation. The Journal of Immunology. 2013; 190(7):3049–3053. [PubMed: 23447690]
11. Nurieva RI, Chung Y, Hwang D, Yang XO, Kang HS, Ma L, et al. Generation of T follicular helper cells is mediated by interleukin-21 but independent of T helper 1, 2, or 17 cell lineages. Immunity. 2008; 29(1):138–149. [PubMed: 18599325]
12. Ray JP, Marshall HD, Laidlaw BJ, Staron MM, Kaech SM, Craft J. Transcription factor STAT3 and type I interferons are corepressive insulators for differentiation of follicular helper and T helper 1 cells. Immunity. 2014; 40(3):367–377. [PubMed: 24631156]
13. Liu X, Chen X, Zhong B, Wang X, Chu F, et al. Transcription factor achaete-scute homologue 2 initiates follicular T-helper-cell development. Nature. 2014; 507(7493):513–518. [PubMed: 24463518]
14. Choi YS, Yang JA, Crotty S. Dynamic regulation of Bcl6 in follicular helper CD4 T (Tfh) cells. Current opinion in immunology. 2013:1–7.
15. Weber BN, Chi AW-S, Chavez A, Yashiro-Ohtani Y, Yang Q, Shestova O, et al. A critical role for TCF-1 in T-lineage specification and differentiation. Nature. 2011; 476(7358):63–68. [PubMed: 21814277]
16. Yu S, Zhou X, Steinke FC, Liu C, Chen S-C, Zagorodna O, et al. The TCF-1 and LEF-1 transcription factors have cooperative and opposing roles in T cell development and malignancy. Immunity. 2012; 37(5):813–826. [PubMed: 23103132]
17. Steinke FC, Xue H-H. From inception to output, Tcf1 and Lef1 safeguard development of T cells and innate immune cells. Immunologic research. 2014; 59(1–3):45–55. [PubMed: 24847765]
18. Steinke FC, Yu S, Zhou X, He B, Yang W, Zhou B, et al. TCF-1 and LEF-1 act upstream of Th-POK to promote the CD4(+) T cell fate and interact with Runx3 to silence Cd4 in CD8(+) T cells. Nature Immunology. 2014; 15(7):646–656. [PubMed: 24836425]
19. Jeannet G, Boudousquié C, Gardiol N, Kang J, Huelsken J, Held W. Essential role of the Wnt pathway effector Tcf-1 for the establishment of functional CD8 T cell memory. Proceedings of the National Academy of Sciences of the United States of America. 2010; 107(21):9777–9782. [PubMed: 20457902]
20. Zhou X, Xue H-H. Cutting edge: generation of memory precursors and functional memory CD8+ T cells depends on T cell factor-1 and lymphoid enhancer-binding factor-1. The Journal of Immunology. 2012; 189(6):2722–2726. [PubMed: 22875805]
21. Zhou X, Yu S, Zhao D-M, Harty JT, Badovinac VP, Xue H-H. Differentiation and persistence of memory CD8(+) T cells depend on T cell factor 1. Immunity. 2010; 33(2):229–240. [PubMed: 20727791]
22. Yu Q, Sharma A, Oh SY, Moon H-G, Hossain MZ, Salay TM, et al. T cell factor 1 initiates the T helper type 2 fate by inducing the transcription factor GATA-3 and repressing interferon-gamma. Nature Immunology. 2009; 10(9):992–999. [PubMed: 19648923]
23. Yu Q, Sharma A, Ghosh A, Sen JM. T cell factor-1 negatively regulates expression of IL-17 family of cytokines and protects mice from experimental autoimmune encephalomyelitis. The Journal of Immunology. 2011; 186(7):3946–3952. [PubMed: 21339363]
24. van Loosdregt J, Fleskens V, Tiemessen MM, Mokry M, van Boxtel R, Meerding J, et al. Canonical Wnt signaling negatively modulates regulatory T cell function. Immunity. 2013; 39(2): 298–310. [PubMed: 23954131]
25. Choi YS, Yang JA, Yusuf I, Johnston RJ, Greenbaum J, Peters B, et al. Bcl6 Expressing Follicular Helper CD4 T Cells Are Fate Committed Early and Have the Capacity To Form Memory. The Journal of Immunology. 2013; 190(8):4014–4026. [PubMed: 23487426]
26. Choi YS, Kageyama R, Eto D, Escobar TC, Johnston RJ, Monticelli L, et al. ICOS Receptor Instructs T Follicular Helper Cell versus Effector Cell Differentiation via Induction of the Transcriptional Repressor Bcl6. Immunity. 2011; 34(6):932–946. [PubMed: 21636296]

27. Pepper M, Pagán AJ, Igyártó BZ, Taylor JJ, Jenkins MK. Opposing signals from the bcl6 transcription factor and the interleukin-2 receptor generate T helper 1 central and effector memory cells. Immunity. 2011; 35(4):583–595. [PubMed: 22018468]

28. Johnston RJ, Choi YS, Diamond JA, Yang JA, Crotty S. STAT5 is a potent negative regulator of TFH cell differentiation. Journal of Experimental Medicine. 2012; 209(2):243–250. [PubMed: 22271576]

29. Eto D, Lao C, Ditoro D, Barnett B, Escobar TC, Kageyama R, et al. IL-21 and IL-6 are critical for different aspects of B cell immunity and redundantly induce optimal follicular helper CD4 T cell (Tfh) differentiation. PloS one. 2011; 6(3):e17739. [PubMed: 21423809]

30. Oestreich KJ, Mohn SE, Weinmann AS. Molecular mechanisms that control the expression and activity of Bcl-6 in T(H)1 cells to regulate flexibility with a T(FH)-like gene profile. Nature Immunology. 2012

31. Chen R, Bélanger S, Frederick MA, Li B, Johnston RJ, Xiao N, et al. In vivo RNA interference screens identify regulators of antiviral CD4(+) and CD8(+) T cell differentiation. Immunity. 2014; 41(2):325–338. [PubMed: 25148027]

32. Vacchio MS, Wang L, Bouladoux N, Carpenter AC, Xiong Y, Williams LC, et al. A ThPOK-LRF transcriptional node maintains the integrity and effector potential of post-thymic CD4+ T cells. Nat Immunol. 2014; 15(10):947–956. [PubMed: 25129370]

33. Zhao D-M, Yu S, Zhou X, Haring JS, Held W, Badovinac VP, et al. Constitutive activation of Wnt signaling favors generation of memory CD8 T cells. The Journal of Immunology. 2010; 184(3): 1191–1199. [PubMed: 20026746]

34. Nance JP, Belanger S, Johnston RJ, Takemori T, Crotty S. Cutting Edge: T Follicular Helper Cell Differentiation Is Defective in the Absence of Bcl6 BTB Repressor Domain Function. Journal of immunology. 2015; 194(12):5599–5603.

35. Tunyaplin C, Shaffer AL, Angelin-Duclos CD, Yu X, Staudt LM, Calame KL. Direct repression of prdm1 by Bcl-6 inhibits plasmacytic differentiation. The Journal of Immunology. 2004; 173(2): 1158–1165. [PubMed: 15240705]

36. Kim SJ, Zou YR, Goldstein J, Reizis B, Diamond B. Tolerogenic function of Blimp-1 in dendritic cells. Journal of Experimental Medicine. 2011; 208(11):2193–2199. [PubMed: 21948081]

37. Lee J-Y, Skon CN, Lee YJ, Oh S, Taylor JJ, Malhotra D, et al. The Transcription Factor KLF2 Restrains CD4(+) T Follicular Helper Cell Differentiation. Immunity. 2015; 42(2):252–264. [PubMed: 25692701]

38. Stone EL, Pepper M, Katayama CD, Kerdiles YM, Lai C-Y, Emslie E, et al. ICOS Coreceptor Signaling Inactivates the Transcription Factor FOXO1 to Promote Tfh Cell Differentiation. Immunity. 2015; 42(2):239–251. [PubMed: 25692700]

39. Pratama A, Srivastava M, Williams NJ, Papa I, Lee SK, Dinh XT, et al. MicroRNA-146a regulates ICOS-ICOSL signalling to limit accumulation of T follicular helper cells and germinal centres. Nature Communications. 2015; 6:6436.

40. Weber JP, Fuhrmann F, Feist RK, Lahmann A, Al Baz MS, Gentz L-J, et al. ICOS maintains the T follicular helper cell phenotype by down-regulating Krüppel-like factor 2. Journal of Experimental Medicine. 2015; 212(2):217–233. [PubMed: 25646266]

41. Vogel KU, Edelmann SL, Jeltsch KM, Bertossi A, Heger K, Heinz GA, et al. Roquin paralogs 1 and 2 redundantly repress the Icos and Ox40 costimulator mRNAs and control follicular helper T cell differentiation. Immunity. 2013; 38(4):655–668. [PubMed: 23583643]

42. Xu H, Li X, Liu D, Li J, Zhang X, Chen X, et al. Follicular T-helper cell recruitment governed by bystander B cells and ICOS-driven motility. Nature. 2013; 496(7446):523–527. [PubMed: 23619696]

43. Batten M, Ramamoorthi N, Kljavin NM, Ma CS, Cox JH, Dengler HS, et al. IL-27 supports germinal center function by enhancing IL-21 production and the function of T follicular helper cells. Journal of Experimental Medicine. 2010; 207(13):2895–2906. [PubMed: 21098093]

44. Poholek AC, Hansen K, Hernandez SG, Eto D, Chandele A, Weinstein JS, et al. In vivo regulation of Bcl6 and T follicular helper cell development. The Journal of Immunology. 2010; 185(1):313–326. [PubMed: 20519643]

45. Harker JA, Lewis GM, Mack L, Zuniga EI. Late Interleukin-6 Escalates T Follicular Helper Cell Responses and Controls a Chronic Viral Infection. Science (New York, NY). 2011; 334(6057): 825–829.

46. Petrovas C, Yamamoto T, Gerner MY, Boswell KL, Wloka K, Smith EC, et al. CD4 T follicular helper cell dynamics during SIV infection. The Journal of clinical investigation. 2012

47. Tubo NJ, Pagán AJ, Taylor JJ, Nelson RW, Linehan JL, Ertelt JM, et al. Single Naive CD4+ T Cells from a Diverse Repertoire Produce Different Effector Cell Types during Infection. Cell. 2013; 153(4):785–796. [PubMed: 23663778]

48. Oxenius A, Bachmann MF, Zinkernagel RM, Hengartner H. Virus-specific MHC-class II-restricted TCR-transgenic mice: effects on humoral and cellular immune responses after viral infection. European Journal of Immunology. 1998; 28(1):390–400. [PubMed: 9485218]

49. Kaji T, Ishige A, Hikida M, Taka J, Hijikata A, Kubo M, et al. Distinct cellular pathways select germline-encoded and somatically mutated antibodies into immunological memory. Journal of Experimental Medicine. 2012; 209(11):2079–2097. [PubMed: 23027924]

50. Choi YS, Crotty S. Retroviral Vector Expression in TCR Transgenic CD4(+) T Cells. Methods in molecular biology (Clifton, NJ). 2015; 1291:49–61.

51. Yusuf I, Kageyama R, Monticelli L, Johnston RJ, Ditoro D, Hansen K, et al. Germinal center T follicular helper cell IL-4 production is dependent on signaling lymphocytic activation molecule receptor (CD150). Journal of immunology. 2010; 185(1):190–202.

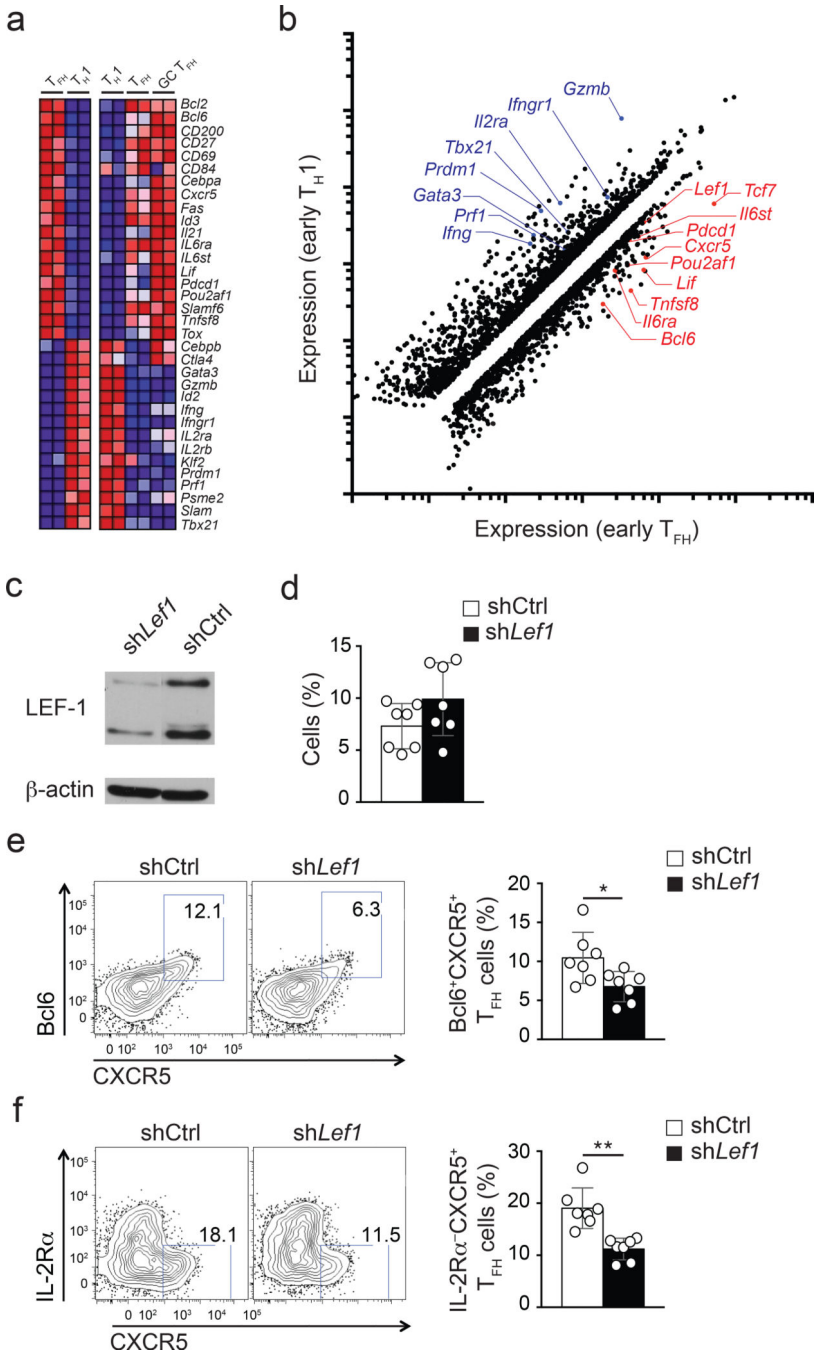

Figure 1. *Lef1* expression is associated with T_{FH} cells and regulates early T_{FH} differentiation

(a) RNA-seq analysis of early T_{FH} (IL-2Rα$^-$Blimp1-YFP$^-$) versus T_H1 (IL-2Rα$^+$Blimp1-YFP$^+$) CD45.1$^+$ Blimp1-YFP SMARTA cells isolated from B6 mice 3 d after SMARTA cell transfer and LCMV infection (left panels), and that of T_H1 (CXCR5$^-$), T_{FH} (PD-1^{lo}CXCR5$^+$), and GC T_{FH} (PD-1^{hi}CXCR5$^+$) sorted 8 d after LCMV from CD45.2$^+$ B6 mice (right panels). Heatmaps of selected genes of interest are shown. **(b)** Scatter plot of genes showing ≥ |1.5 fold| differential expression in early T_{FH} in comparison to T_H1 cells. Select genes of interest are marked. **(c)** Immunoblot of LEF-1 (two isoforms) and β-actin

from sh*Ctrl*$^+$ and sh*Lef1*$^+$ SMARTA cells. **(d-f)** Analysis of sh*Ctrl*$^+$ or sh*Lef1*$^+$ CD45.1$^+$ SMARTA cells (Ametrine$^+$CD45.1$^+$CD4$^+$CD19$^-$), three days after transfer of shRNA-RV-infected SMARTA cells into B6 mice and LCMV infection. **(d)** shRNA$^+$ SMARTA cell frequency among total CD4$^+$ T cells. **(e-f)** Phenotyping of sh*Ctrl*$^+$ and sh*Lef1*$^+$ SMARTA cells. (**e**) Bcl6$^+$CXCR5$^+$ T_{FH} cells. **(f)** IL-2Rα$^-$CXCR5$^+$ T_{FH} cells. Quantitation shown as % of SMARTA cells (mean ± s.e.m.). Data are a composite of two independent experiments (n = 7 per group). * $P < 0.05$, ** $P < 0.001$ (Student's *t*-test).

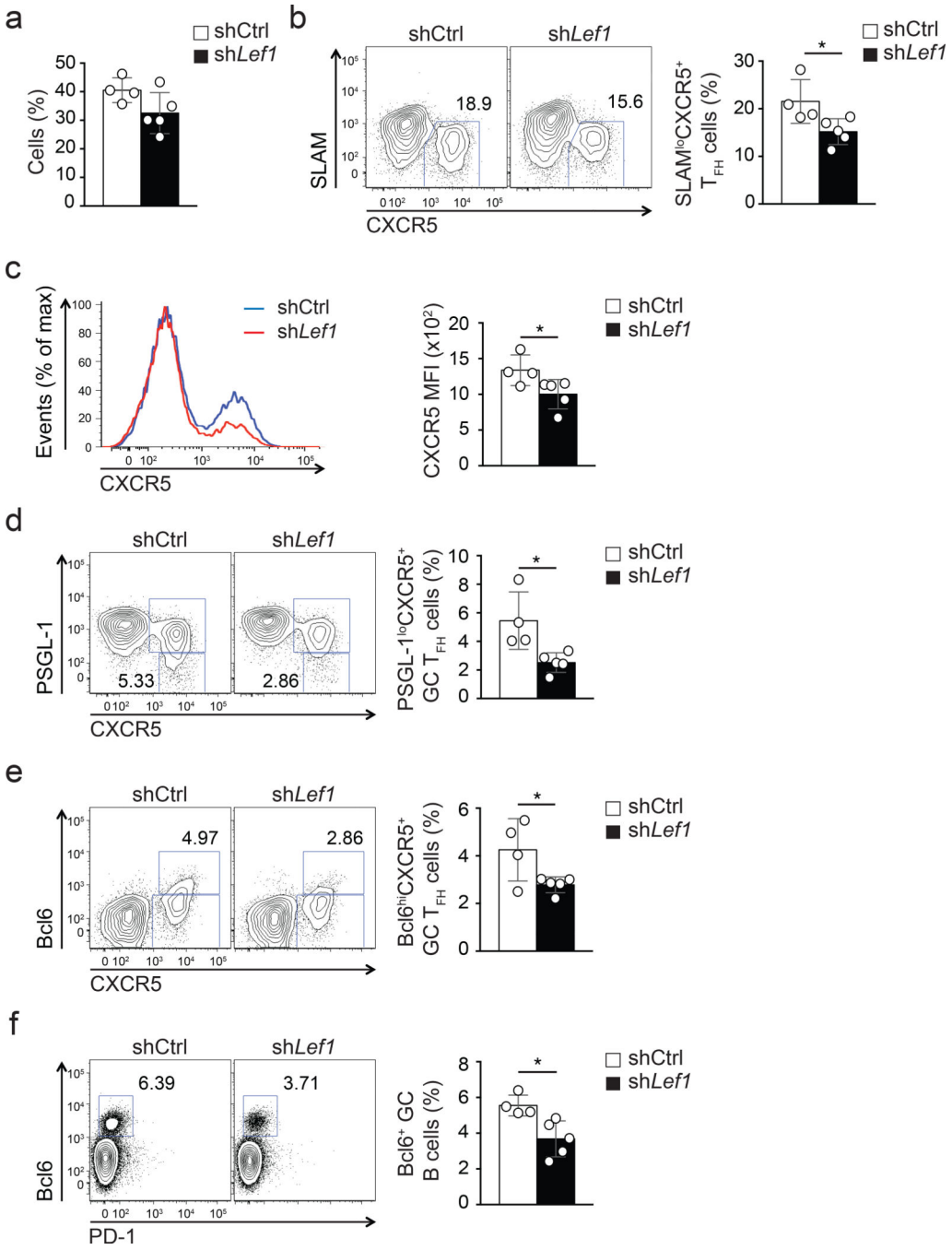

Figure 2. LEF-1-dependent T_{FH} differentiation supports germinal center responses

(**a-e**) Frequencies and phenotypes of sh*Ctrl*$^{+}$ or sh*Lef1*$^{+}$ CD45.1^{+} SMARTA cells assessed by flow cytometry at 8 d after SMARTA cell transfer into B6 mice and LCMV infection. **(a)** Abundance of shRNA^{+} SMARTA cells (Ametrine^{+}CD45.1^{+}CD4^{+}CD19^{-}) among total CD4^{+} T cells. **(b)** Frequency of SLAM^{lo}CXCR5^{+} T_{FH} cells. Quantitation shown as % of SMARTA cells. **(c)** Expression of CXCR5 on sh*Ctrl*$^{+}$ (blue) and sh*Lef1*$^{+}$ (red) SMARTA cells. **(d-e)** Frequencies of sh*Ctrl*$^{+}$ and sh*Lef1*$^{+}$ SMARTA GC T_{FH} cells among SMARTA cells phenotyped as PSGL-1^{lo}CXCR5^{+}**(d)** and Bcl6^{hi}CXCR5^{+} (**e**). **(f)** Abundance of GC B

cells ($Bcl6^{+}CD19^{+}$) among total B cells. Data are representative of two independent experiments (n = 4–5 per group, mean ± s.e.m.). * $P < 0.05$ (Student's *t*-test).

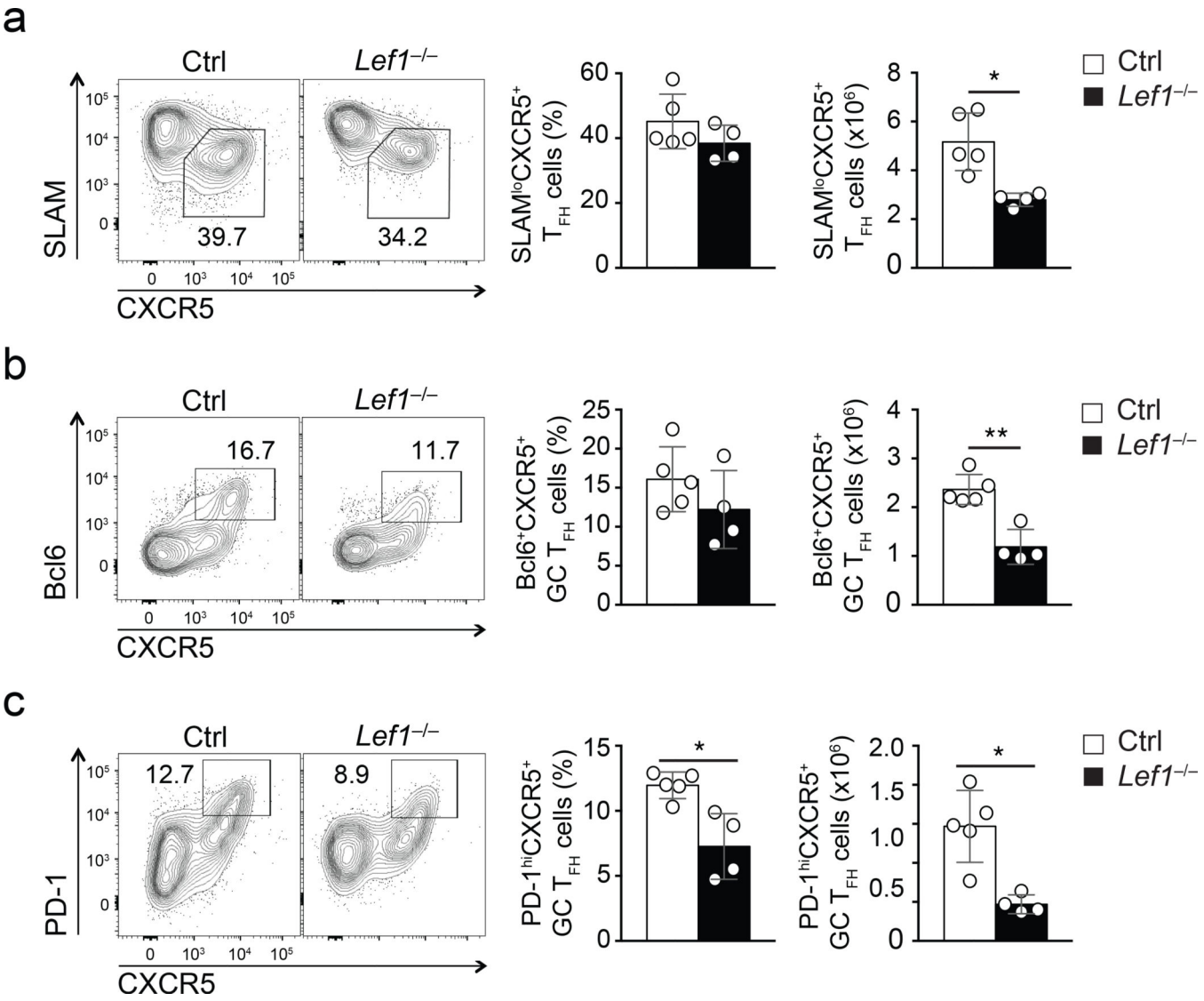

Figure 3. Genetic ablation of LEF-1 impairs GC T_{FH} differentiation

(**a-c**) Flow cytometry of T_{FH} and GC T_{FH} cells in spleens of *Lef1*$^{-/-}$ mice and littermate controls infected *w*ith vaccinia virus for 8 days. Plots are gated on CD44^{hi}CD62L^{lo}GFP^{+}CD4^{+} T cells. **(a)** SLAM^{lo}CXCR5^{+} T_{FH} cells. (**b-c**) Abundance of GC T_{FH} cells phenotyped as Bcl6^{+}CXCR5^{+} (**b**) and PD-1^{hi}CXCR5^{+}**(c)**. Cumulative data from four independent experiments are shown (mean ± s.d.). * $P < 0.01$, ** $P < 0.001$ (Student's *t*-test).

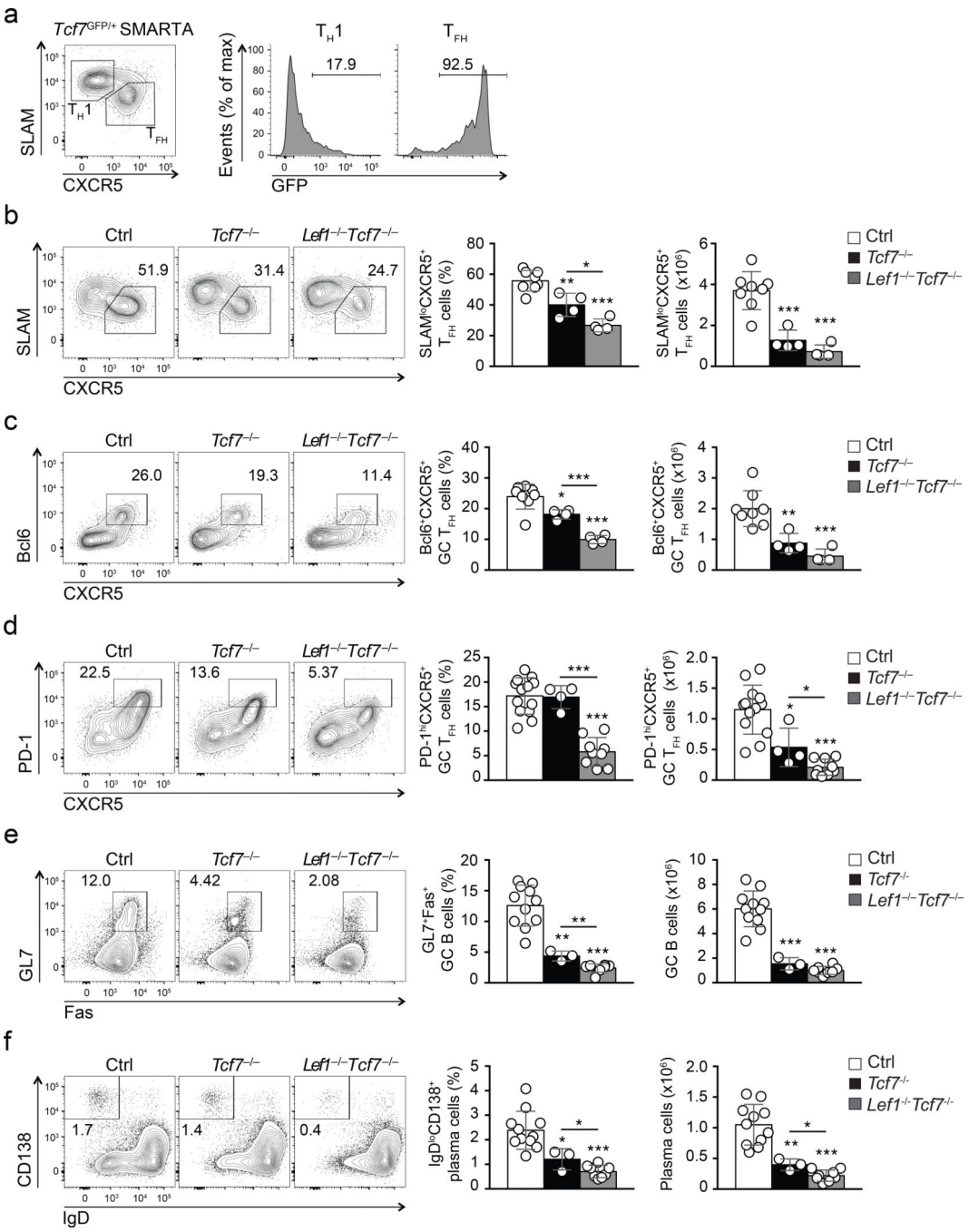

Figure 4. Both TCF-1 and LEF-1 contribute to regulation of T_{FH} differentiation and B cell responses

(a) Flow cytometry of *Tcf7*-GFP expression in SMARTA CD4$^+$ T cells (CD45.2$^+$CD4$^+$) at 8 d after *Tcf7*$^{GFP/+}$ SMARTA cell transfer into CD45.1$^+$ recipients and LCMV infection. Gated populations of T_H1 (CXCR5$^-$SLAM^{hi}) and T_{FH} (CXCR5$^+$SLAM^{lo}) cells were analyzed for *Tcf7*-GFP expression. Numbers indicate percent *Tcf7*-GFP$^+$ cells. Data are representative of ≥ 2 experiments. **(b-f)** Flow cytometry of *Tcf7*$^{-/-}$*Lef1*$^{-/-}$*Tcf7*$^{-/-}$, and littermate controls 8 d after infection *i.v.* with vaccinia virus. **(b-d)** Abundance of

$SLAM^{lo}CXCR5^{+}$ T_{FH} cells **(b)**, $Bcl6^{+}CXCR5^{+}$ GC T_{FH} cells **(c)**, and $PD\text{-}1^{hi}CXCR5^{+}$ GC T_{FH} cells **(d)** gated on $CD44^{hi}CD62L^{-}GFP^{+}CD4^{+}$ T cells in spleen. (**e-f**) Abundance of $GL7^{+}Fas^{+}$ GC B cells **(e)** and $IgD^{lo}CD138^{+}$ plasma cells **(f)** in the same animals (mean ± s.d.). Cumulative data from ≥ 3 experiments are shown. * $P < 0.05$, ** $P < 0.01$, *** $P < 0.001$ (Student's *t*-test).

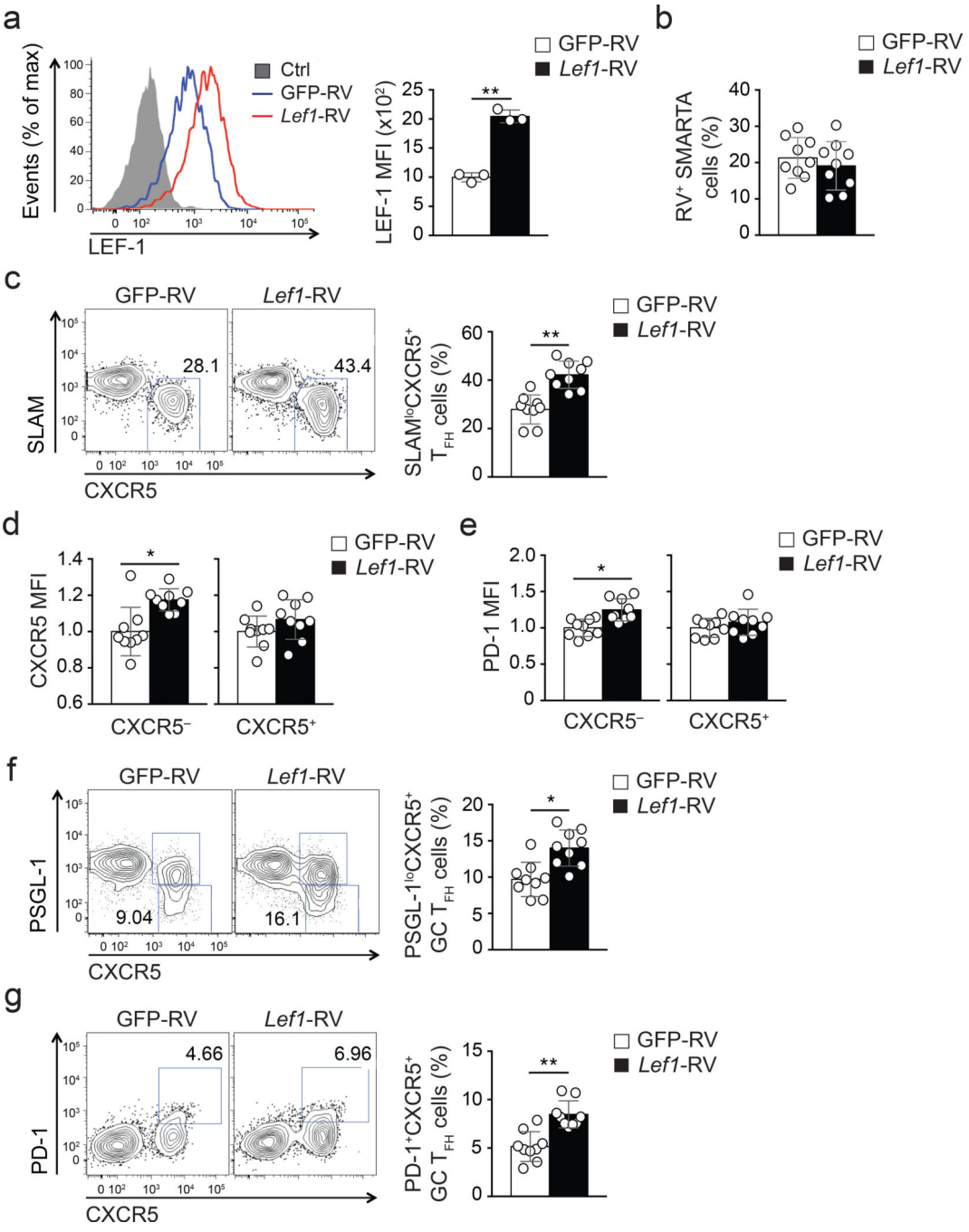

Figure 5. Enhanced *Lef1* expression leads to augmented T_{FH} differentiation

(a) Expression of LEF-1 in GFP-RV$^+$ (blue) and *Lef1*-RV$^+$ (red) SMARTA cells assessed by flow cytometry. **(b-g)** Frequencies and phenotypes of GFP-RV$^+$ or *Lef1*-RV$^+$ SMARTA cells (CD45.1$^+$CD4$^+$CD19$^-$) assessed by flow cytometry at 8 d after SMARTA cell transfer into B6 mice (CD45.2$^+$) and LCMV infection. **(b)** Abundance of RV$^+$ SMARTA cell (GFP$^+$CD45.1$^+$CD4$^+$CD19$^-$) among total CD4$^+$ T cells. **(c)** Abundance of SLAM^{lo}CXCR5$^+$ T_{FH} cells among RV$^+$ SMARTA cells. **(d-e)** Expression of canonical T_{FH} markers CXCR5 **(d)** and PD-1 **(e)** on CXCR5$^-$ T_H1 and CXCR5$^+$ T_{FH} cells by *Lef1*-RV$^+$ and GFP-RV$^+$ cells,

normalized to the mean MFI per group (mean ± s.e.m.). **(f-g)** Abundance of GC T_{FH} cells phenotyped as PSGL-1^{lo}CXCR5^{+}**(f)** and PD-1^{hi}CXCR5^{+}**(e)** of RV^{+} SMARTA cells. Data are a composite of two independent experiments (n = 9 per group). * $P < 0.01$, ** $P < 0.001$ (Student's *t*-test).

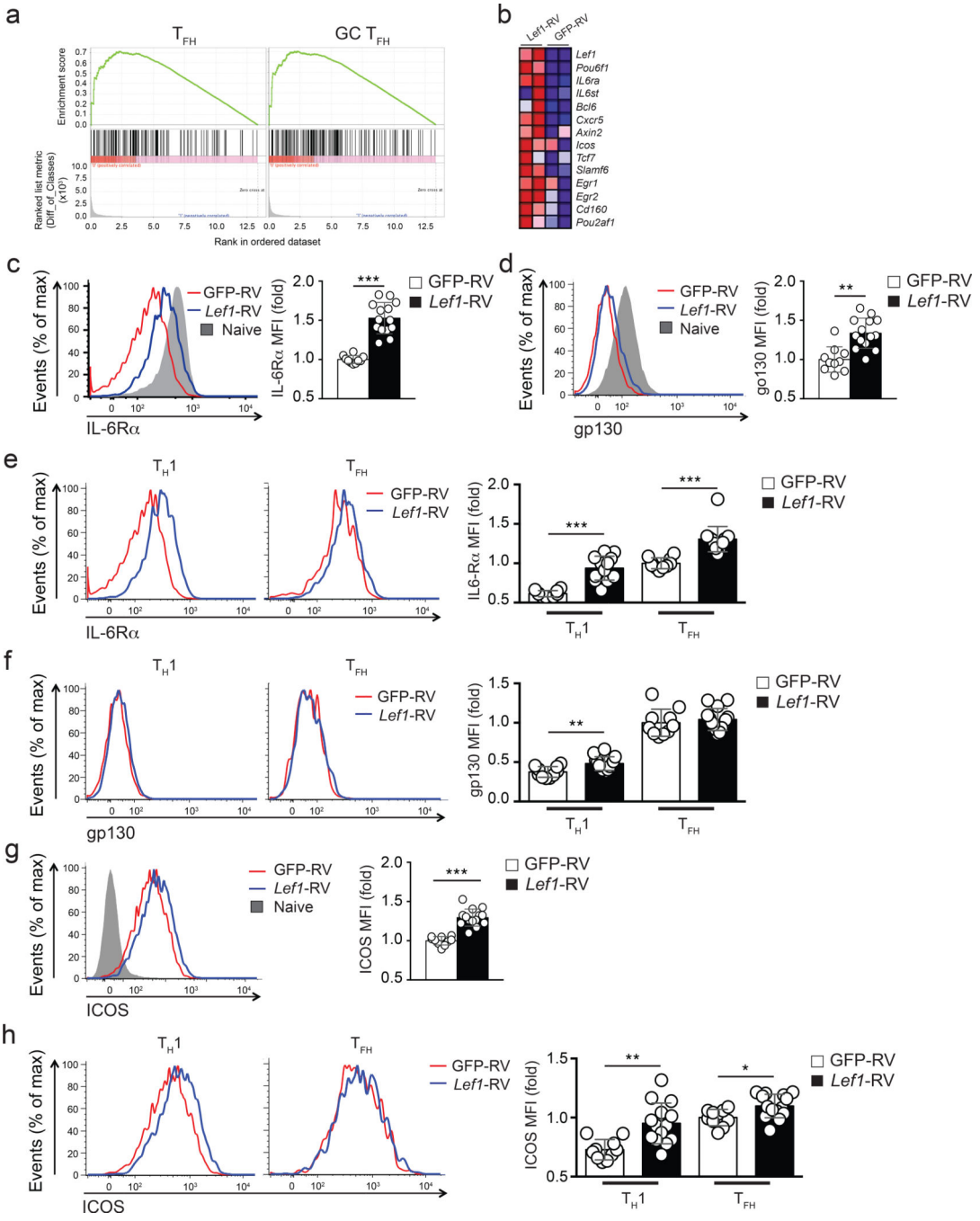

Figure 6. LEF-1 regulates expression of IL-6 receptor chains and ICOS

(a-b) RNA-seq analysis of GFP-RV$^+$ and *Lef1*-RV$^+$ SMARTA cells (CD45.1$^+$CD4$^+$CD19$^-$) sorted into CXCR5$^+$ T_{FH} or CXCR5$^-$ T_H1 populations isolated from B6 mice 4 d after SMARTA cell transfer and LCMV infection. **(a)** GSEA enrichment analysis showing enrichment of T_{FH} and GC T_{FH} gene signatures in *Lef1*-RV$^+$ T_H1 cells compared to GFP-RV$^+$ T_H1 cells. **(b)** Heat map of selected genes upregulated in *Lef1*-RV$^+$ T_H1 cells compared to GFP-RV$^+$ T_H1 cells. **(c-h)** Flow cytometry of GFP-RV$^+$ or *Lef1*-RV$^+$ SMARTA cells (CD45.1$^+$CD4$^+$CD19) assessed at 3 d after SMARTA cell transfer into B6 mice (CD45.2$^+$)

and LCMV infection. (**c-d**) Expression of IL6Rα **(c)** and gp130 **(d)** on RV^+ SMARTA cells. **(e-f)** Comparative expression of IL-6Rα (**e**) and gp130 (**f**) GFP-RV^+ (red) and *Lef1*-RV^+ (blue) T_H1 and T_{FH} cells. (**g-h**) Abundance of ICOS on total RV^+ SMARTA cells **(g)**, $CXCR5^+$ T_{FH} and $CXCR5^-$ T_H1 cell subpopulations **(h)** in the same animal (mean ± s.e.m.). Data are a composite of three independent experiments (n = 10–14 per group). * $P < 0.05$, ** $P < 0.01$, *** $P < 0.001$ (Student's *t*-test).

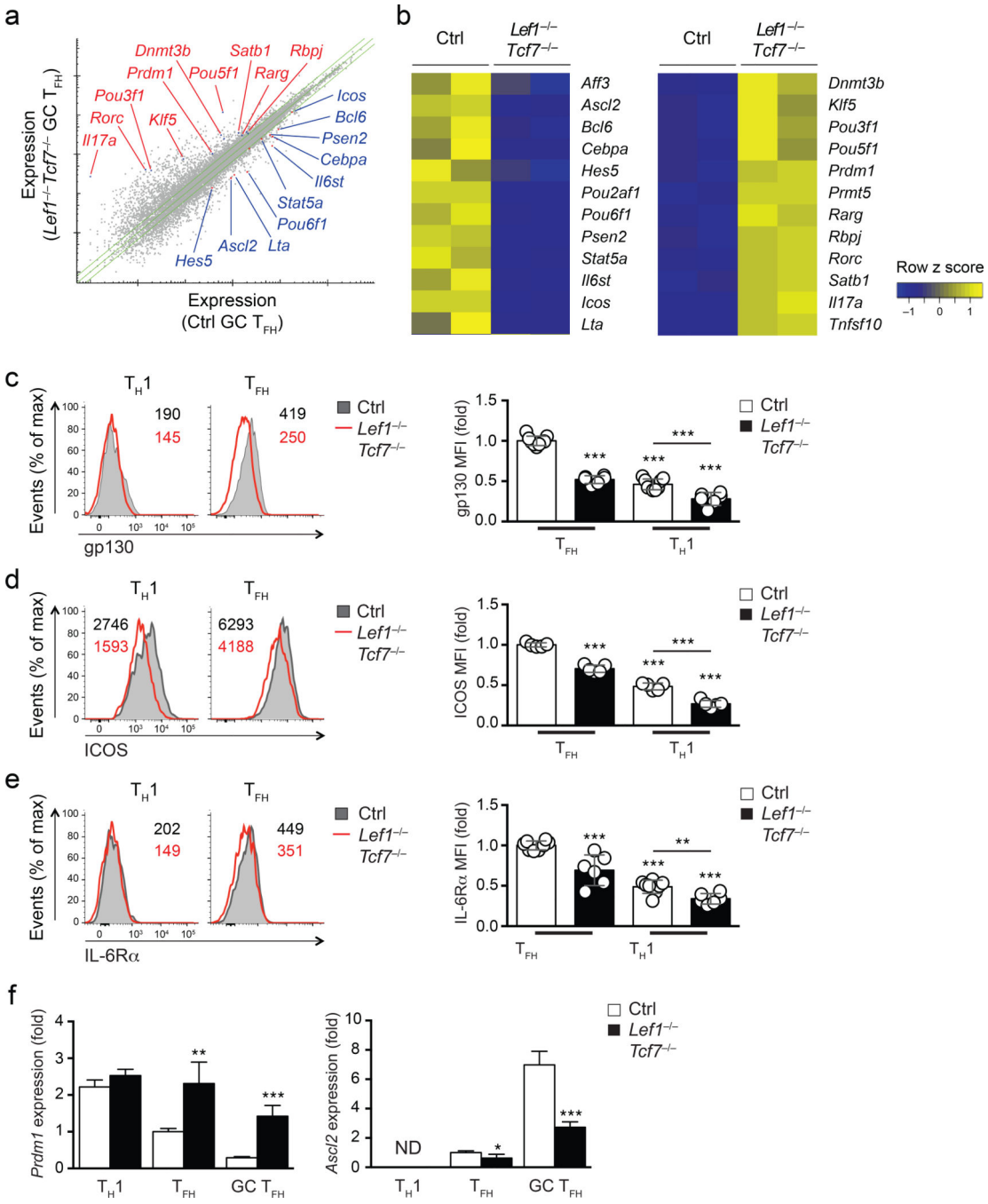

Figure 7. LEF-1 and TCF-1-dependent transcriptional regulation of T_{FH}-related genes

(a) RNA-seq analysis of PD-1^{hi}CXCR5^{+} GC T_{FH} cells sorted from spleens of *Lef1*$^{-/-}$*Tcf7*$^{-/-}$ and littermate controls 8 d after vaccinia virus infection. Green lines mark mean gene expression of ≥ |1.5 fold| differences. Select genes of interest are marked. **(b)** Heatmap of selected differentially regulated genes between control and *Lef1*$^{-/-}$*Tcf7*$^{-/-}$ GC T_{FH} cells. **(c-e)** Flow cytometry of *Lef1*$^{-/-}$*Tcf7*$^{-/-}$ and littermate controls 8 d after infection *i.v.* with vaccinia virus. CXCR5^{+} T_{FH} and CXCR5^{-} T_H1 cells were analyzed for gp130 **(c)**, ICOS **(d)**, and IL-6Rα **(e)** expression (mean ± s.d.). Bar graphs are normalized to the mean

MFI on control T_{FH} cells. Data are a composite of 4 independent experiments (n = 5–9 per group). **(f)** Gene expression of *Ascl2* and *Prdm1* was determined by quantitative RT-PCR in $CXCR5^{-}$ T_H1, PD-$1^{lo}CXCR5^{+}$ T_{FH}, and PD-$1^{hi}CXCR5^{+}$ GC T_{FH} cells sorted from *Lef1*$^{-/-}$*Tcf7*$^{-/-}$ and littermate controls 8 d after infection *i.v.* with vaccinia virus. Data are from 2 experiments with each sample measured in duplicate and normalized to control T_{FH} cells. ND, not reliably detected. * $P < 0.05$, ** $P < 0.01$, *** $P < 0.001$ (Student's *t*-test).

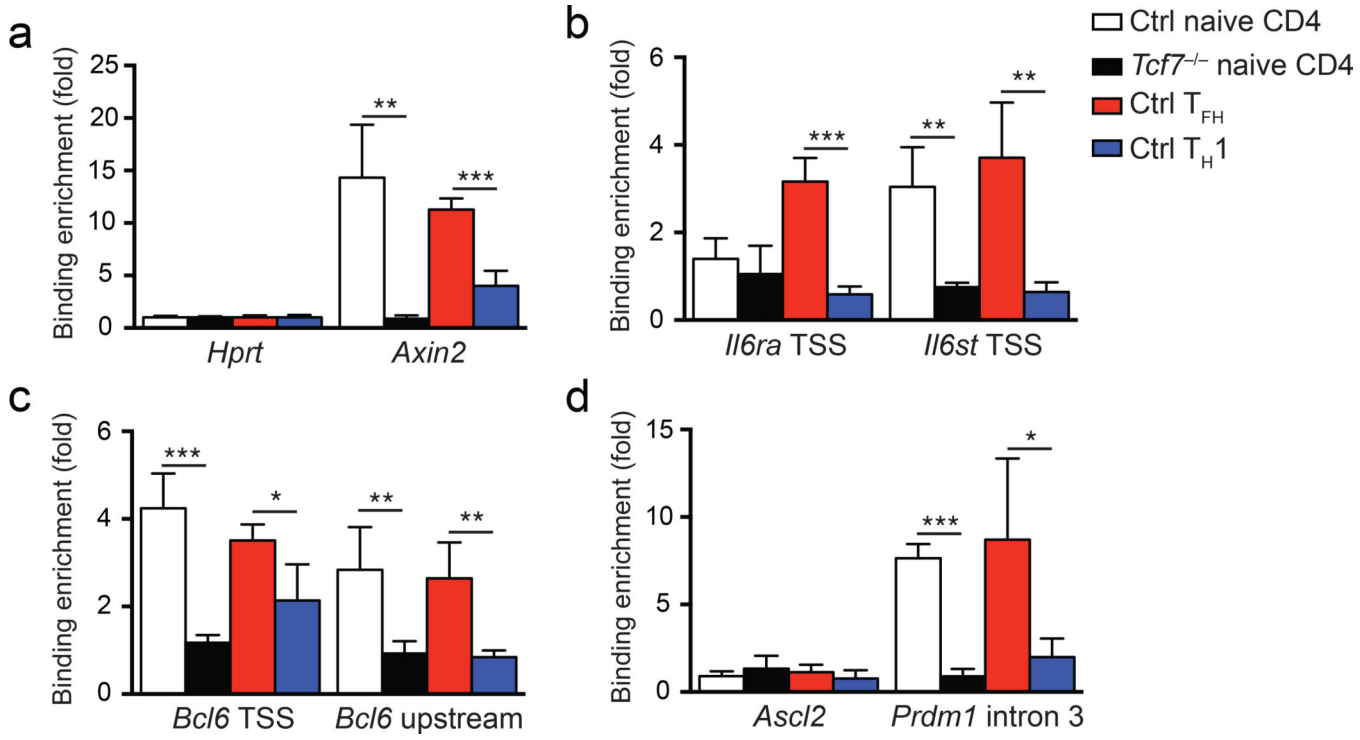

Figure 8. TCF-1 binds to key T_{FH}-associated genes in T_{FH} cells

(a-d) ChIP assays using anti-TCF-1 antibody or control IgG were performed on naive control $CD4^+$ T cells ($CD44^{lo}CD62L^+CD4^+$); naive *Tcf7*$^{-/-}$ $CD4^+$ T cells ($GFP^+CD44^{lo}CD62L^+CD4^+$); WT T_{FH} cells ($CXCR5^+CD44^{hi}CD62L^-CD4^+$); and WT T_H1 cells ($CXCR5^-CD44^{hi}CD62L^-CD4^+$). T_{FH} and T_H1 cells were sorted from B6 mice 8 d after vaccinia virus infection. Quantitation of enriched TCF-1 binding was done at the positive control *Axin2* gene **(a)**, the TSS of the *Il6ra* and *Il6st* genes **(b)**, the TSS and a −2.8 kb upstream regulatory region of the *Bcl6* gene **(c)**, and the TSS of *Ascl2* and intron 3 of *Prdm1* **(d)**, and data are means ± s.d. from 3 independent experiments. * $P < 0.05$, ** $P < 0.01$, *** $P < 0.001$ (Student's *t*-test).